

*Початку третього тисячоліття  
присвячується*

*Началу третього тисячелеття  
посвящается*

*To the Beginning of the Third Millennium*

УДК 539.3

© 2003

J. Awrejcewicz, A. V. Krysko

## WAVELETS-BASED ANALYSIS OF PARAMETRIC VIBRATIONS OF FLEXIBLE PLATES

**1. Introduction.** The term 'wavelet' has appeared relatively late, i. e. in eighties Grossman and Morlet [1] introduced this term with respect to their investigation of seismic and acoustic signals. Nowadays, a family of analyzing tools called 'wavelets' is often used to solve the following problems: image recognition; signal synthesis (for instance, human speech signals); various representations (rainbow, kidney X-ray photograph, satellite representation of clouds or a planet surface, photos of materials, etc.); analysis of properties of turbulent flow; solutions to equations; packing of large amount of informations, and other.

Note that the wavelet analysis of one dimensional signal refers to its decomposition with respect to a basic somehow similar to a soliton-like function (wavelet) obtained via its scale and shift transformations. Each of the basic functions represents both a frequency as well as a spatial localization. Therefore, the wavelet transformation yields two dimensional signal representation, where time and frequency are considered as the independent values. *In result one gets an opportunity to analyse signal properties simultaneously in time and in frequency domains.*

The above mentioned properties can be generalized into multi dimensional signals (or functions). Note that an application of wavelets is not limited to that of signal and different fields properties obtained either numerically or experimentally. Wavelets are used for numerical modeling as a hierarchic basis suitable for description of a nonlinear processes characterizing interaction of spatial and time scales. In particular, the wavelet analysis serves as a very good tool to investigate essentially non-homogeneous processes, since its basic elements are well localized and include a 'moving' frequency-time window.

Very often it is also referred as a 'mathematical microscope', since very good results are obtained for different scales.

Many examples show how suitable is this 'microscope' owing to investigation of the internal structure of an analysed object. We briefly mention examples of fractal Weierstrass functions or probabilistic measures of Cantor series, or an application of wavelet analysis into a turbulent velocity field in the wind channel for large Reynolds numbers. In fact, the latter one proved an occurrence of Richardson's cascade. Also, a convergence of energetic cascade process with a structure of multi-fractal invariant measures has been shown for some well known dynamical systems modeling observed scenarios leading to chaos in dissipative systems.

The nonlinear and chaotic behaviours in the time-frequency domain is analysed using wavelet-transform in reference [2]. It is shown that the wavelet-transform isolates weak sub-harmonics or higher-harmonics from the fundamental harmonic response, and that it easily yields the random property of chaotic response and both phase in time and frequency domain responses. A five degree-of-freedom Duffing's structural system is studied.

Alves [3] proposed an efficient stable and accurated multiresolution adaptive approach combined with high-resolution methods to trace a solution either of a single or a system of partial differential equations.

Multi-scale singular-spectrum analysis is applied for a wavelet optimization in the time frequency domain in reference [4]. Several examples of application to synthetic signals with fractal or power-law behaviour are studied.

An application of wavelet transforms to the recognition and visualization of characteristic features of speech and of music sounds is proposed in reference [5].

Computations of decaying two-dimensional turbulence in an adaptive wavelet basis are reported in reference [6]. The new presented algorithm includes two main terms: operator-adapted test functions and the adaptive evolution of the convection term. It has been shown that turbulent flows can be approximated with a reduced number of degrees of freedom.

Two-dimensional parabolized Navier - Stokes equations governing an increase of convection are studied using a wavelet regularization approach in reference [7]. Neglecting the small-scale wavelet coefficients a control dimension is essentially reduced, among others.

A new algorithm based on the wavelet representation of the space of approximation, is proposed to study the 1D periodic and regularized Burgers equation [8]. The exponential decay of the spline wavelets in the physical and Fourier spaces allows for both handling the differential operators and working with very flexible orthogonal and numerically well localized functions.

Two wavelet indices, both multiscale accumulative density and variation, are proposed in reference [9] for the characterization of spatiotemporal patterns. Numerical experiments based on the Cahn - Hilliard equation indicate the efficiency of the proposed approach.

Two spatiotemporal chaotic systems of complex Ginzburg - Landau oscillators with diffusive and non-local interactions are studied using wavelets in reference [10].

The wavelet projections of one-dimensional Kuramoto - Sivashinsky equation are studied in reference [11], and various localized relatively low-dimensional examples of spatiotemporal chaos are reported.

The wavelets procedures are successfully applied to the field of mechanics. For instance, fractal and wavelet theory is applied to study a chaotic behaviour [12]. A wavelet based selection procedure to detect faults in multi-degrees-of-freedom systems and to approximate the impulse response of those systems is addressed in references [13, 14]. Coca and Billings [15] used wavelet decomposition to identify of both linear and non-linear systems. A wavelet logarithmic decrement formula is introduced to detect damping in multi-degree-of-freedom systems from time-domain responses [16]. A wavelet-based procedure proposed in reference [17] allows both the parameter estimation of a priori known dynamical models as well as the identification of classes of suitable non-linear models using input-output data. In reference [18] the wavelet transform is applied to traffic measurements and its multiplicative character is demonstrated. Luo et al. studied vibration modelling using fast Gaussian wavelet algorithm [19]. Wavelet analysis is used to study a stability of one-degree-of-freedom system subjected to non-conservative forces [20]. The wavelet expansions of the stresses across the shell thickness is proposed to trace deformations of thin elastoplastic structures in reference [21]. A continuous wavelet transform is applied to estimate Lyapunov exponents in reference [22].

The Galerkin - wavelet procedure to trace solutions of ordinary differential equations with T-periodic coefficients as a wavelet series expansion of T-periodic wavelet [23] using a Poisson periodization technique [24] is proposed in reference [25]. The method inherits fundamental wavelets properties (localization, universal approximation of very general signals and operators) and a real multiresolution approach to analyse parametrically excited systems. Recall that the theory of multiresolution approach developed by Mallat [26, 27] represents a suitable frame work providing Hilbertian bases of spaces  $L^2(\mathbb{R})$  and  $L^2(\mathbb{R}/T\mathbb{Z})$  [28].

To sum up, wavelets can be satisfactorily applied to analysis of many qualitatively different problems. In this work the wavelet theory is used to analyse complex parametric vibrations of flexible plates.

Various models governing nonlinear dynamics of plates and shells possess their own history and they still require a rigorous mathematical treatment. For example, we briefly mention the von Kármán equation considered in the cited reference [29]. Finite dimensionality and compactness of attractors for von Kármán equation are considered by Lasiecka [30]. More generalized questions are also addressed in references [31, 32]. The von Kármán model is analysed in this paper applying the wavelet-based approach.

In spite of some new results devoted to bifurcation and chaos exhibited by the investigated thin infinite length plate dynamics, another one important problem is discussed. Note that usually the partial differential equations governing behaviour of continuous systems are transformed to a nonlinear set of ordinary differential equations using the Bubnov - Galerkin procedure without a This question is illustrated and discussed in the paper, and in

addition the finite difference method is applied which gives 'almost' exact results [33, 34], and hence it serves as a tool for a validity estimation of higher order Bubnov - Galerkin procedures. rigorous motivation and the error estimation. This question is illustrated and discussed in the paper, and in addition the finite difference method is applied which gives 'almost' exact results [33, 34], and hence it serves as a tool for a validity estimation of higher order Bubnov - Galerkin procedures.

The paper is organized in the following way. In Sect. 1 an analogy between the Fourier and wavelet series is described. The wavelet transformation and its properties are presented and discussed (our presentation is on a basis of the material covered in the monographs [35 - 44] and the references [46 - 52]). In the Sect. 2 the results of wavelet analysis to investigate chaotic vibrations of flexible plates sinusoidally and longitudinally loaded are presented. Brief concluding remarks finish the paper contents.

**2. Theory.** In this section, definitions and properties related to wavelet analysis are overviewed for one dimensional functions. However, one may extend the consideration to multi-dimensional cases.

**2.1. 1. From Fourier to wavelet transformation.** Both integral Fourier transformation and Fourier series are used to carry out the harmonic analysis. The yielded Fourier coefficients have a relatively simple physical interpretation. All of the properties can be derived using only two real functions  $\sin t$ ,  $\cos t$  or the complex one  $\exp(it) = \cos(t) + i \sin(t)$ ,  $i^2 = -1$ .

The wavelet analysis is applied relatively recently and its mathematical background is still under construction. Therefore, following [36] the necessary definitions of wavelet analysis are introduced with a simultaneous reference to the classical Fourier analysis.

**Fourier series.** First we introduce some notations which will be used further. Let  $L^2(0, 2\pi)$  be the space of squared integrable functions with finite energy

$$\int_0^{2\pi} |f(t)|^2 dt < \infty \quad t \in (0, 2\pi).$$

In fact, this is a definition of piecewise continuous function  $f(t)$ . It can be periodically extended and defined in the whole real axis  $R(-\infty, \infty)$ , such that  $f(t) = f(t - 2\pi)$  holds for every  $t$  from  $R$ . An arbitrary  $f(t)$ , taken from the space of  $2\pi$ -periodical and squared integrable functions, can be represented by the Fourier series  $f(t) = \sum_{-\infty}^{\infty} c_n \exp(int)$ , with the coefficients

$$c_n = (2\pi)^{-1} \int_0^{2\pi} f(t) \exp(-int) dt.$$

The series is uniquely converged to  $f(t)$ , i. e.

$$\lim_{M, N \rightarrow \infty} \int_0^{2\pi} \left| f(t) - \sum_M^N c_n \exp(int) \right|^2 dt = 0.$$

Note that  $w_n(t) = \exp(int)$ ,  $n = \dots, -1, 0, 1, \dots$  creates the orthonormal basis of the space  $L^2(0, 2\pi)$  constructed with a help of a scale shift of the one function  $w(t) = \exp(it)$  in such a way that  $w_n(t) = w(nt)$ .

Any of  $2\pi$ -periodic squared integrable functions can be obtained by a superposition of scale transformations of the basic or mother wavelet function  $w(t) = \exp(it) = \cos(t) + i \sin(t)$ . In words, it is a composition of sinusoidal waves with different frequencies and with coefficients depending on the harmonics number (frequency).

Recall that for the Fourier coefficients the following Parseval's formula holds

$$(2\pi)^{-1} \int_0^{2\pi} |f(t)|^2 dt = \sum_{-\infty}^{\infty} |c_n|^2.$$

2.1.2. *Wavelet series.* Consider the space  $L^2(R)$  of the functions  $f(t)$  with the finite energy defined on the whole real axis  $R(-\infty, \infty)$   $E_f = \int_0^{2\pi} |f(t)|^2 dt < \infty$ .

The functional spaces  $L^2(0, 2\pi)$  and  $L^2(R)$  are essentially different. In particular, a local average value of each function from  $L^2(R)$  should approach zero on  $\pm\infty$ . Since a sinusoidal wave does not belong to  $L^2(R)$ , a family of sinusoidal waves  $w_n$  can not be a basic of the functional space  $L^2(R)$ .

Let us try to find relatively simple functions which can be used to the basic construction of the space  $L^2(R)$ .

Observe that 'waves' creating the space  $L^2(R)$  should tend to zero on  $(\pm\infty)$  in a rather fast way. Let us take well localized soliton-like 'small waves' as the basis functions. We are going to construct the functional space  $L^2(R)$  using only one wavelet  $\psi(t)$ , in a way similar to that of the space  $L^2(0, 2\pi)$  with one basic function  $\psi(t)$ .

The question arises, how one may cover the whole axis  $R(-\infty, \infty)$  using a fastly tending to zero localized function. It can be done applying a set of shifts along the axis. For simplicity, we assume the integer shifts, i.e.  $\psi(t - k)$ .

A similar like definition of a sinusoidal frequency can be introduced using powers of two:  $\psi(2^j t - k)$ , where  $j, k$  are integers ( $j, k \in I$ ).

In what follows using scale transformations  $(1/2^j)$  and shifts  $(k/2^j)$  all of the frequencies can be defined, and hence the whole axis can be covered having only one basis wavelet  $\psi(t)$ .

Recall the norm definition

$$\|p\|_2 = \langle p, p \rangle^{1/2}, \quad \langle p, p \rangle = \int_{-\infty}^{\infty} p(t) \bar{q}(t) dt,$$

where the bar denotes a complex conjugate value. Consequently, the following relation holds:  $\|\psi(2^j t - k)\|_2 = 2^{-j/2} \|\psi(t)\|_2$ . Therefore, if any wavelet  $\psi(t) \in L^2(R)$  possesses a unit norm, it follows that all wavelets of the family  $\{\psi_{jk}\}$  of the dyadic form

$$\psi_{jk}(t) = 2^{j/2} \psi(2^j t - k), \quad (j, k \in I), \quad (2.1)$$

are also normalized to one, i. e.  $\|\psi_{jk}\|_2 = \|\psi\|_2 = 1$ .

A wavelet  $\psi(t) \in L^2(R)$  is said to be orthogonal, if the family  $\{\psi_{jk}\}$  defined in (2.1) is the orthonormalized basis of the functional space  $L^2(R)$

$$\langle \psi_{jk}, \psi_{lm} \rangle = \delta_{jk} \delta_{lm},$$

and any  $f \in L^2(R)$  can be represented by the series

$$f(t) = \sum_{j,k=-\infty}^{\infty} c_{jk} \psi_{jk}(t), \quad (2.2)$$

which is uniformly convergent in  $L^2(R)$ :

$$\lim_{M_1, N_1, M_2, N_2 \rightarrow \infty} \left\| f - \sum_{-M_2}^{N_2} \sum_{-M_1}^{N_1} c_{jk} \psi_{jk} \right\|_2 = 0.$$

One of the simplest wavelet example is the HAAR-wavelet defined in the following way

$$\psi^H(t) = \begin{cases} 1, & 0 \leq t < 1/2, \\ -1, & 1/2 \leq t < 1, \\ 0, & t < 0, t \geq 1. \end{cases} \quad (2.3)$$

It is not difficult to check that any two functions  $\psi_{jk}^H, \psi_{jm}^H$  obtained from  $\psi^H(t)$  using the formula (2.1) and the scale transformations  $(1/2^j), (1/2^j)$  and shifts  $(k/2^j), (m/2^j)$  are orthogonal and possess the unit norm.

Now, we are going to construct a basis of the functional space  $L^2(R)$  using scale transformations and shifts of the wavelet applying arbitrary values of the basis parameters: the scale coefficient  $a$  and the shift parameter  $b$

$$\psi_{ab}(t) = |a|^{-1/2} \psi((t-b)/a), \quad a, b \in R, \quad \psi \in L^2(R). \quad (2.4)$$

Also, the following integral wavelet-transformation is defined

$$[W_\psi f](a, b) = |a|^{-1/2} \int_{-\infty}^{\infty} f(t) \bar{\psi}((t-b)/a) dt = \int_{-\infty}^{\infty} f(t) \bar{\psi}_{ab}(t) dt. \quad (2.5)$$

Extending the discussed analogy to the Fourier transformation one may define the coefficients  $c_{jk} = \langle f, \psi_{jk} \rangle$  of the series (2.2) of the function  $f$  into the wavelet series via the wavelet-transformation  $c_{jk} = [W_\psi f](1/2^j, k/2^j)$ .

Note that further, instead of  $[W_\psi f](a, b)$  used to define the coefficients (amplitudes) of the wavelet-transformation, we use  $W(a, b)$  or  $W_\psi f$  or  $W[f]$ .

To conclude, any function from  $L^2(R)$  can be obtained by a superposition of scale transformation and shifts of the mother wavelet. In words, it is a composition of 'small waves' with coefficients depending on the wave number (frequency, scale) and depending on the shift parameter (time).

An application of the discrete wavelet transformation (discrete frequency-time space in the form of integer shifts and extensions with respect to powers of two) yields the proofs of many results from the wavelet theory [23, 36 - 38] including those of basis orthogonality, series convergence, and so on. The mentioned proofs are often necessary. For instance, during compression of informations or in the modeling problems, i. e. everywhere when after the series of transformations one requires an exact formula of the inversed transformation.

In general, a continuous wavelet transformation is much more suitable to analyse various signals.

**2.1.3. Inversed wavelet transformation.** A sinusoidal wave represents an orthonormalized basis of the functional space  $L^2(0, 2\pi)$  and there is not a problem to find an inversed transformation. The orthonormalized basis of the space  $L^2(R)$  depends on the choice of basis wavelet and a way of basis construction (i. e., on the values of basic parameters-shift and scale coefficients).

Note that a wavelet may be considered as the basis function  $L^2(R)$  only in the case if the yielded by this wavelet basis is orthonormalized and an inverse transform exists. However, the rigorous proofs of orthogonality are rather tedious (see, for instance, references [23, 36 - 38]). Besides, for practical purposes the so called 'almost' basis wavelets are often used.

Here we refer to the inversed transformations only in two cases: for the basis (1), allowing for extensions and shifts  $(1/2^j, 1/2^k)$ ,  $j, k \in I$ , and for the basis (4), obtained for the arbitrary values  $(a, b)$ ,  $a, b \in R$ .

For a given basis parameters  $(a, b)$ ,  $a, b \in R$ , an inversed wavelet transformation is defined using the same basis transformation (4), i. e.

$$f(t) = C_\psi^{-1} \iint [W_\psi f](a, b) \psi_{ab}(t) da db / a^2,$$

where  $C_\psi$  is the normalized coefficient (analogous to the coefficient  $(2\pi)^{1/2}$ , which normalizes

the Fourier transformation)  $C_\psi = \int_{-\infty}^{\infty} |\hat{\psi}(\omega)|^2 |\omega|^{-1} d\omega < \infty$ , where hat denotes the Fourier image.

Observe that the Fourier transform  $\hat{\psi}(0) = 0$ , and also that  $\int_{-\infty}^{\infty} \psi(t) dt = 0$ .

It happens often that only positive frequency values (i. e. for  $a > 0$ ) are considered. A wavelet satisfies the following condition

$$C_\psi = 2 \int_0^{\infty} |\psi^\wedge(\omega)|^2 \omega^{-1} d\omega = 2 \int_0^{\infty} |\psi^\wedge(-\omega)|^2 \omega^{-1} d\omega < \infty.$$

In addition, the so called stable basis for the discrete wavelet transformation can be defined using the following steps.

The function  $\psi(t) \in L^2(\mathbb{R})$  is called R-function, if the basis  $\{\psi_{jk}\}$ , defined by (2.1), is the Riesz basis in the sense that two constants  $A, B$  ( $0 < A \leq B < \infty$ ) exist for which the following inequality

$$A \|\{c_{jk}\}\|_2^2 \leq \left\| \sum_{j=-\infty}^{\infty} \sum_{k=-\infty}^{\infty} c_{jk} \psi_{jk} \right\|_2^2 \leq B \|\{c_{jk}\}\|_2^2$$

holds for any bounded series with the property

$$\|\{c_{jk}\}\|_2^2 \leq \sum_{j=-\infty}^{\infty} \sum_{k=-\infty}^{\infty} |c_{jk}|^2 < \infty.$$

For any R-function there exists the basis  $\{\psi_{jk}\}$ , representing number 2 of the basis  $\{\psi_{jk}\}$ , in the sense that  $\langle \psi_{jk}, \psi_{lm} \rangle = \delta_{jk} \delta_{lm}$ , and the following approximation holds

$$f(t) = \sum_{j,k=-\infty}^{\infty} \langle f, \psi_{jk} \rangle \psi_{jk}(t).$$

If  $\psi$  is the orthogonal wavelet and  $\{\psi_{jk}\}$  is the orthonormed basis, then  $\{\psi_{jk}\}$  overlap and formula (6) becomes the inversed formula. If  $\psi$  is non-orthonormed wavelet but is dyadic wavelet, then it has the partner  $\{\psi^*\}$ , which is used to construct a dyadic family  $\{\psi_{jk}^*\}$  similarly to the basis (2.1)

$$\psi_{jk}^*(t) = \psi^*(t) = 2^{j/2} \psi^*(t) = (2^j t - k), \quad j, k \in I.$$

In a general case, the reconstructional formula (6) does not necessarily becomes a wavelet series in the sense that  $\psi$  is not a wavelet and  $\{\psi_{jk}^*\}$  may not have dyadic basis constructed using (2.4).

**2.1.4. Frequency-time localization.** The Fourier transformation and the Fourier series are widely applied to analyse various processes. Any real signal belongs to  $L^2(\mathbb{R})$ . The Fourier transformation of a signal  $f(t)$  having finite amount of energy defined by the norm  $\|f\|_2$  represents a spectrum of this signal, i. e.

$$f^\wedge(\omega) = \int_{-\infty}^{\infty} f(t) e^{-i\omega t} dt.$$

However, it appears that a physical interpretation of the mentioned formula is sometimes not obvious. Hence, in order to get a spectral information with regard to a given frequency one needs to know all previous and future information. This formula does not contain the required information. In words, it does not take into account a potential evolutionary changes of frequency.

Besides, it is well known that a signal frequency is inversely proportional to its duration. Therefore, in order to get information on a high frequency part, one should take relatively small time intervals instead of taking the whole signal length into considerations. And vice versa, a low frequency spectral information can be obtained using rather wide time intervals.

A part of the mentioned drawbacks is omitted applying the so called window Fourier transformation. However, an infinite oscillating basis function (sinusoidal wave), does not allow to obtain a localized information. An element of a basis of the wavelet transformation fastly tends to zero outside of a short interval and the so called 'localized spectral analysis' can be carried out. In words, the wavelet analysis inherently includes moving frequency-time window, which is automatically narrow on small scales and wide on large scales.

Since both wavelet  $\psi$  and its Fourier transform  $\psi^\wedge$  quite fast overlap with each other, they can be used as the 'window functions' with a 'center' and 'width' defined in the following way.

For any non-trivial window like function  $z(t) \in L^2(\mathbb{R})$  (it is necessary that  $tz(t)$  also belongs to  $L^2(\mathbb{R})$ ), its center  $t^*$  and radius  $\Delta_z$  are defined by the following formulas

$$t^* = \left( \frac{1}{\|z\|_2^2} \int_{-\infty}^{\infty} t |z(t)|^2 dt \right)^{1/2} \quad \text{and} \quad \Delta_z = \left( \frac{1}{\|z\|_2^2} \int_{-\infty}^{\infty} (t - t^*)^2 |z(t)|^2 dt \right)^{1/2}.$$

A width of the window function is equal to  $2\Delta_z$ .

Let  $t^*$ ,  $\Delta_\psi$ ,  $\omega^*$ ,  $\Delta_{\psi^\wedge}$  are the centers and radiuses of a wavelet  $\psi$  and its Fourier transform  $\psi^\wedge$ , respectively. Then the integral wavelet transformation (2.5) is bounded by the 'time window'

$$[win_t] = [b + at^* - 2a\Delta_\psi, b + at^* + 2a\Delta_\psi].$$

In words, the time localization with the window centre in  $b + at^*$  and window width  $2a\Delta_\psi$  takes place. Given the function  $\eta(\omega) = \psi^\wedge(\omega + \omega^*)$ , which is also a window like function with a centre equal to zero and the radius  $\Delta_{\psi^\wedge}$ . Using the formula  $\langle f, g \rangle = \langle f^\wedge, g^\wedge \rangle / 2\pi$ , the integral wavelet transformation (2.5) of the Fourier transform  $f^\wedge$  can be cast in the following way

$$W(a, b) = |a|^{1/2} \int_{-\infty}^{\infty} f^\wedge(\omega) e^{ib\omega} \overline{\eta}\left(a(\omega - \omega^*/a)\right) d\omega. \quad (2.7)$$

If one omits a phase shift and a constant, then it is clear that the transformation of the spectrum  $f^\wedge(\omega)$  of the signal  $f(t)$  with a 'frequency window' has the form

$$[win_\omega] = [\omega^*/a - \Delta_{\psi^\wedge}/a, \omega^*/a + \Delta_{\psi^\wedge}/a].$$

A frequency localization takes place in a vicinity of the window centre  $\omega^*/a$  with the window width  $2\Delta_{\psi^\wedge}/a$ .

Observe that a ratio of central frequency over a window width

$$(\omega^*/a) / (2\Delta_{\psi^\wedge}/a) = \omega^* / (2\Delta_{\psi^\wedge})$$

does not depend on location of a central frequency, and the frequency-time window  $[win_t] \times [win_\omega]$ , having the surface  $4\Delta_\psi \Delta_{\psi^\wedge}$  becomes narrow (wide) for high (low) central frequency  $\omega^*/a$  (Fig. 1, a).

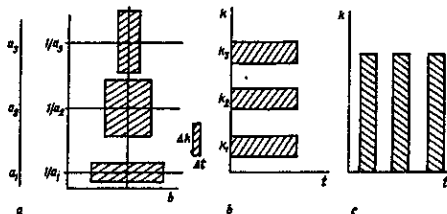


Fig. 1

In Fig. 1, a, a localization in frequency-time space of the Fourier (Fig. 1, b) and Shannon (Fig. 1, c) transformations are reported. It is known, that the Fourier transform of a series with equal discretization in time  $\Delta t$  can not achieve higher discretization than  $\Delta\omega = \Delta t / 2$  (recall a Nyquist frequency exhibiting a principle of undeterminism between time and frequency localization). Analogous boundness for the wavelet transformation can be expressed by the inequality  $\Delta t \Delta\omega \geq 1/(4\pi)$ . It is seen from Fig. 1 that the Fourier transform very well localizes frequency but without time localization; the Shannon transformation does not possess frequency localization; wavelet transformation has a moving window localized in a vicinity of chosen time instant and widening with a scale increase, which is the most required property for obtaining a spectral information.

Now we are going to compare the wavelet transformation (2.5) with often used short-time Fourier transformation

$$F(\omega, b) = \int f(t) z(t - b) e^{i\omega t} dt,$$

where  $z$  is the window type function. Observe that  $F(\omega, b)$  represents a signal development with respect to a family of the functions  $z(t - b)e^{i\omega t}$ , which is constructed using one function  $z(t)$  with a help of shifts  $b$  in time and the shifts  $\omega$  with respect to frequency. On the other hand, the wavelet transformation  $W(a, b)$  is the series development of a signal with respect to the family  $\psi((t - b)/a)$ , created by the one function  $\psi(t)$  with a help of shifts  $b$  in time and the extensions  $a$  also in time. In words, wavelet-transformation represents a continuous set of window like Fourier transformations with different windows for each frequency.

It means that the basic functions of a window Fourier transformation have one and only one solution in time and frequency ( $z(t), z^*(\omega)$ ) for all points of plane mapping, whereas the basic functions of the wavelet-transformation have decreasing with scale time function  $\psi(t/a)$  and increasing with scale frequency function  $\psi^*(a\omega)$ . This property of the wavelet-transformation yields many advantages during signal analysis, since high frequency characteristics correspond to low frequency signal part.

One may expect that the described advantages of wavelets can be very useful during solutions of equations.

**2.2. Basic functions of wavelet transformation.** Up to now wavelet is treated as a certain soliton like function with the described properties. Since there is a lack of a general wavelet definition, we focused on wavelet characteristic features. Note that a majority of limitations introduced for wavelets are caused by a requirement of inversed transformation.

**2.2.1. Wavelet characteristic features.** We list some necessary properties which are required by a function in order to be a wavelet.

**Localization.** A wavelet transformation (contrary to the Fourier transformation) uses the localized basis function. The wavelet should be localized both in time and frequency domains.

$$\text{Zero average value} \quad \int_{-\infty}^{\infty} \psi(t) dt = 0.$$

It often appears, that all first  $m$  moments are required to be zero (so called  $m$ -th order wavelet)

$$\int_{-\infty}^{\infty} t^m \psi(t) dt = 0.$$

$M$ -th order wavelets, ignoring mostly regularized polynomial parts of a signal, are especially suitable for analysis of small scale fluctuations and higher order singularities.

$$\text{Boundeness} \quad \int |\psi(t)|^2 dt < \infty.$$



An estimation of a proper localization and boundness can be obtained in the form  $|\psi(t)| < 1/(1 + |t|^n)$  or  $|\psi^\wedge(\omega)| < 1/(1 + |k - \omega_0|^n)$ , where  $\omega_0$  is the dominant wavelet frequency, and  $n$  should be possibly large.

**Self-similarity.** This property belongs to most important wavelet features. All of wavelets of the family  $\psi_{ab}(t)$  have the same number of oscillations as mother wavelet  $\psi(t)$ , since all of them are obtained from  $\psi(t)$  using series of scaling and shifts.

Now we consider some examples from references [23, 49]. There are three functions being wavelets (three last examples), and three functions which are not wavelets (three first examples). In Fig. 2, there are functions depending on time (first row) and their Fourier images (second row).

Note that a good localized in  $t$ -space  $\delta$  function loses this property in  $k$ -space (Fig. 2, a). A good localized in  $k$ -space sinus is not localized in  $t$ -space (Fig. 2, b). Recall that the Gabor function (Fig. 2, c)

$$G(t) = \exp[i\Omega(t - t_0) - i\nu] \exp[-(t - t_0)^2 / 2\sigma^2] / [\sigma(2\pi)^{1/2}]$$

is the modulated Gauss function with four parameters: shift  $t_0$ , standard averaged squared deviation  $\sigma$ , modulation frequency  $\Omega$  and phase shift  $\nu$ . A development into the Gabor series refers to development into the modulated parts of a sinusoid. Since the length of all frequencies is the same and constant, it gives different number of oscillations for different harmonics. In words, good localized Gabor functions in both  $k$  and  $t$  spaces do not exhibit a self-similarity property.

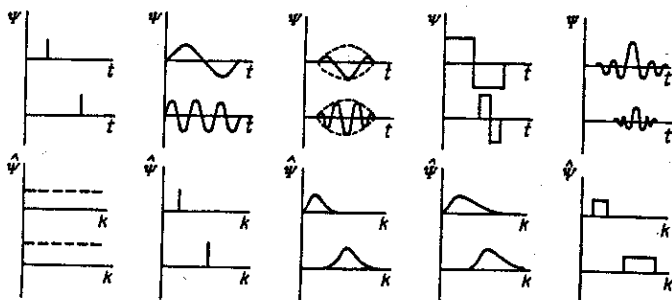


Fig. 2

HAAR-wavelet (formula (1.3), Fig. 2, d) is an example of orthogonal discrete wavelet with orthonormed basis.

One of its main drawback is that of piece-wise linear components in  $t$ -space, which causes an occurrence of infinite (decreasing of  $k^{-1}$  order) tails in  $k$ -space, as well an asymmetry of the form. However, in some applications those drawbacks are not essential and even in some cases this behaviour can be treated as advantages. Often a symmetric FHAT-wavelet (French hat) is applied, which is governed by the formula

$$\psi(t) = \begin{cases} 1, & |t| \leq 1/3, \\ -1/2, & 1/3 < |t| \leq 1, \\ 0, & |t| > 1, \end{cases} \quad \psi^\wedge(k) = 3H(k)(\sin k/k - \sin 3k/3k),$$

where:  $H(k)$  is the Heviside function.

In Fig. 2, e the so called LP-wavelet is reported (Littlewood, Paley). Contrary to the FHAT wavelet, which is irregular in time space and slowly decreasing in frequency domain, the LP-wavelet possesses strictly exhibited boundaries in the Fourier space and more wash out boundaries in time domain.

Both mentioned wavelets may be treated as the limiting ones and one can find a more suitable wavelet located between them (their properties).

2.2.2. *Examples of wavelet functions.* Since the wavelet transformation is represented by a scalar product of analyzing wavelet and a being analysed signal, the coefficients  $W(a, b)$  include a combined information on the wavelet and on the signal (similar to the Fourier coefficients possessing information on a signal and on a sinusoidal wave). A choice of a wavelet depends on a required information to be extracted from a signal. Each of wavelets has characteristic singularities in time and frequency domains, and hence using different wavelets one may detect and exhibit various properties of the analysed signal.

Recalling a comparison to a 'mathematical microscope', observe that the shift parameter  $b$  fixes the microscope focus, the scale coefficient  $a$  exhibits the enlargement, and finally, a choice of basis wavelet  $\psi$  is defined by optical microscope properties.

The real bases are often constructed using derivatives of the Gauss function

$$\psi_m(t) = (-1)^m \partial_t^m \left[ \exp(-|t|^2/2) \right], \quad \hat{\psi}_m(k) = m(it)^m \exp(-|k|^2/2),$$

where  $\partial_t^m = \partial^m [ ] / \partial t^m$ . Higher derivatives allow to detect information of higher order singularities of a signal, since they give zero moments.

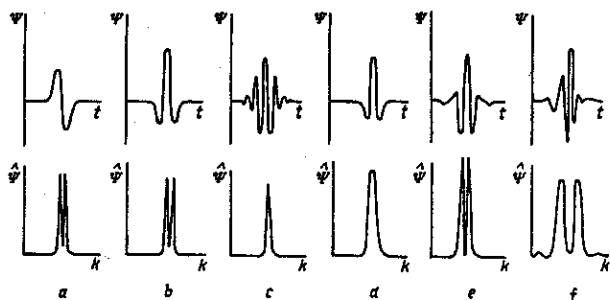


Fig. 3

In Fig. 3a, b the wavelets for  $m = 1$ ,  $m = 2$  are shown, respectively. The first one is called WAVE-wavelet, whereas the second is called MHAT-wavelet (Mexican hat).

Since the MHAT-wavelet has a narrow energy spectrum and two zero moments, it is well suitable to analyse complex signals. MHAT can be generalized to two dimensional case, and it can be used to analyse isotropic fields. If one takes a derivative in one direction, a non-isotropic basis with "good angle properties" is obtained [49]. In order to construct such basis, one has to add a rotation to scale and shift transformations. In result, the 'mathematical microscope' has also polarization properties with the polarization angle proportional to the rotation wavelet angle.

Applying Gauss functions, one obtains the well known DOG-wavelet (difference of Gaussians)

$$\psi(t) = \exp(-|t|^2/2) - 0,5 \exp(-|t|^2/8),$$

$$\hat{\psi}(k) = (2\pi)^{-1,2} \left[ \exp(-|k|^2/2) - \exp(-2|k|^2) \right].$$

Examples of complex wavelets are reported in Fig. 3c, d (only their real parts are shown).

Often applied complex basis is constructed using well localized (in both  $k$  and  $t$  domains) Morlet wavelet [1] defined by the formulas

$$\psi(t) = \exp(it_0 t) \exp(-t^2/2), \quad \hat{\psi}(k) = H(k) \exp[-(k - k_0)^2/2],$$

which describes a flat wave modulated by Gaussian of unit width. In Fig. 3c, the Morlet wavelet for  $k_0 = 6$  is shown. When  $k_0$  is increased, the angle basis properties are improved, but the space basis properties are worsed.

The Pauli [50] wavelet

$$\psi(t) = \Gamma(m+1)i^m / (i-it)^{m+1}, \quad \psi_m^{\wedge}(k) = H(k)(k)^m \exp(-k)$$

is often applied in quantum mechanics and it is shown in Fig. 3d for  $m = 4$ . Increase of  $m$  enlarges number of wavelet zero moments. The presented complex wavelets are progressive. The latter have zero value Fourier coefficients for negative values of wave numbers. They are well adapted for signals for which causality is valid; they conserve a time direction and they do not introduce the parasite interference between past and future.

Note that during analysis of complex one dimensional signal or during application of complex analyzing wavelet, in output one gets two dimensional massive values of moduli of coefficients and phase  $W(a, b) = |W(a, b)| \exp(i\Phi(a, b))$ .

In Fig. 3e, f, examples of wavelets often used for construction of orthogonal discrete bases of type (1) using Mallat procedure [26, 27] are reported: LMB-wavelet (Lemarié, Meyer, Battle) [46, 53] and on of the Daubechies wavelets [23].

**2.3. Properties and application of wavelet transformation.** Contrary to one-dimensional Fourier transformation, yielding also one dimensional information about a relative contributions (amplitudes) of different scales (frequencies), a wavelet transformation of one dimensional series is two dimensional amplitudes massive of wavelet transformation-the values of coefficients  $W(a, b)$ . A distribution of these values in the space  $(a, b) = (\text{time scale, time localization})$  gives information on evolution of a relative contribution of structures of different scale in time and is called (analogously to the amplitude spectrum or Fourier coefficients) the spectrum of wavelet transformation coefficients, frequency-or time-scale spectrum, or wavelet spectrum. To distinguish between the classical Fourier spectrum, the latter is referred to be single spectrum.

**2.3.1. Presentation of results.** A spectrum  $W(a, b)$  of one-dimensional signal represents a surface in three dimensional space. One may use various ways of information visualization. Besides the surfaces, often their projection into the  $(a, b)$  plane with isoclines or grey intensity pictures, where one may trace wavelet transformation amplitudes, change in time and frequency domains, as well as graphs of local extremum of those surfaces (the so called skeleton).

Since a rather wide scale interval is required, the  $(\log a, b)$  coordinates are recommended.

**2.3.2. Properties of wavelet transformation.** The coefficients of wavelet transformation include combined information on analysed wavelet and signal. In spite of this drawback, the wavelet transformation yields on objective information of a being analysed signal, since certain wavelet properties do not depend on the wavelet choice. This is a very important property.

The fundamental elementary properties of wavelet transformation of the function  $f(t)$  follow (the following notations are applied  $[W_{\psi} f](a, b) = W(f) = W(a, b)$ ).

1<sup>o</sup>. *Linearity*

$$W[\alpha f_1(t) + \beta f_2(t)] = \alpha W[f_1] + \beta W[f_2] = \alpha W_1(a, b) + \beta W_2(a, b).$$

It means that a wavelet transformation of a vector function yields a vector with components being a wavelet transformation of each of the analysed vector components separately.

2<sup>o</sup>. *Shift invariance.*

$$W[f(t - b_0)] = W(a, b - b_0).$$

This yields commutativity of differentiation, and in particular  $\partial_t W[f] = W[\partial_t f]$ , where one gets a transpositions also for derivatives of the vector.

3<sup>0</sup>. Extension (stretching) invariance.

$$W[f(t/a_0)] = (1/a_0)W(a/a_0, b/a_0).$$

This property is used to detect singularities of the analysed function.

The cited properties do not depend on a choice of analyzing wavelet. Other important properties follow.

1<sup>1</sup>. Time-Frequency localization and occurrence of time-frequency window and an angle of influence (one may use the term scale-time localization). The parameters of a time-frequency window are given in Sect. 2.1.4.

2<sup>1</sup>. Differentiation.

$$W[\partial_t^m f] = (-1)^m \int_{-\infty}^{\infty} f(t) \partial_t^m [\bar{\psi}_{ab}(t)] dt.$$

It means that after differentiation a function or a wavelet gives the same result.

Note that often a function  $f$  is composed of series of numbers, whereas wavelet is given by a formula.

3<sup>1</sup>. For a wavelet transformation an analog of the Parseval's theorem holds, i.e.

$$\int f_1(t) \bar{f}_2(t) dt = C_{\psi^{-1}} \iint W_1(a, b) \bar{W}_2(a, b) da db / a^2.$$

It means that signal energy can be calculated via amplitudes (coefficients) of wavelet transformation similarly to the Fourier transformation:

$$E = \int f^2(t) dt = \int |A(\omega) - iB(\omega)|^2 d\omega.$$

It should be emphasized, that definitions and properties of continuous one dimensional wavelet transformation can be easily generalized into multi dimensional and discrete cases. However, these problems are omitted here.

2.3.3. Wavelet analysis possibilities. Having wavelet spectra, many useful characteristics and properties of a being analysed process can be reconstructed. We briefly describe how to analyse a signal singularities and its energetic characteristics.

a) Local regularity [47, 49].

Consider certain implications of scale invariance 3<sup>0</sup>.

If  $f \in C^m(t_0)$ , i. e. a being analysed function is continuously differentiable up to order  $m$  in the point  $t_0$ , then the coefficients of wavelet transformation for  $t = t_0$  should satisfy the inequality  $W(a, t_0) \leq a^{m+1/2}$  for  $a \rightarrow 0$ .

The multiplier  $a^{1/2}$  occurs, since due to scale invariance 3<sup>0</sup>, the skeleton properties of the function  $f$  have to be investigated using  $L^1$ -normalized coefficients. Recall, that  $L^1$ - and  $L^2$ -normalized coefficients are coupled via simple relation  $W(a, t_0) \leq a^{-1/2} W(a, b)$ .

If  $f \in \Lambda^\alpha(t_0)$ , i. e. the analysed function belongs to Holder space of the functions  $\alpha$  (in words,  $f$  is continuous but not necessarily differentiable in  $t_0$ , but  $|f(t+t_0) - f(t)| = c|t_0|^\alpha$ ,  $\alpha < 1$ ,  $c = \text{const} > 0$ ), then the coefficients of its wavelet transformation for  $t = t_0$  should satisfy the relation  $W(a, t_0) \approx ca^\alpha a^{1/2}$  for  $a \rightarrow 0$ .

A wavelet transformation is composed in such a way that even for a not-regular function  $f(t)$ , the  $W(a, b)$  is regular. Whole potential information on  $f(t)$  singularities ( $t_0$  localization,  $c$  intensity,  $\alpha$  exponent) is exhibited by an asymptotic behaviour of the coefficients  $W(a, t_0)$  for small  $a$ . If the coefficients on the small scales are divergent, then  $f$  has a singularity in  $t_0$  and the singularity exponent  $\alpha$  is defined by the inclination angle

$\log|W(a, t_0)|$  to  $\log a$ . In contrary, if the coefficients are located in zero vicinity in a neighbourhood of  $t_0$  on small scales, hence  $f(t)$  is regular in the point  $t_0$ .

Note that the described property is often used to analyse fractal and multifractal signals [39, 45], since a typical property of fractals sets is their self-similarity. In words, watching for  $f$  in a vicinity of  $t_0$  with different scales, we practically observe this function on different scales:  $f(\lambda t + \lambda t_0) - f(\lambda t) \approx \lambda^{\alpha(t_0)}(f(t + t_0) - f(t))$ . Transformation basis is self-similar. It is not difficult to show, that the transformation coefficients are scaled with the same exponent, as that of the analysed function:  $W(\lambda a, t_0 + \lambda b) \approx \lambda^{\alpha(t_0)}W(a, t_0)$ . This property serves to find the skeleton exponent  $\alpha(t_0)$ , which measures fractal dimension of a set. Analysis of multi-fractal sets yields a spectrum of exponents and a spectrum of dimensions.

Note also that analysis of a local regularity is universal in some sense, since it does not depend on the wavelet choice.

Energy characteristics [48, 49].

We consider some consequences of the property for a wavelet transformation implies that in space of real functions, the full energy of the  $3^1$ .

An existence of the Parsivale's analog signal  $f$  can be described via amplitudes of the Wavelet-transformation of the form

$$E_f = \int f^2(t) dt = C_w^{-1} \iint W^2(a, b) da db / a^2.$$

A density of the signal energy  $E_w(a, b) = W^2(a, b)$  characterizes energy levels (excitation levels) of a being analysed signal  $f(t)$  in the space  $(a, b) = (\text{scale, time})$ .

Local energy spectrum. One of the peculiar property of the wavelet transformation is the possibility to investigate localized characteristics and investigate local properties of processes.

Knowing density of energy  $E_w(a, b)$ , one may define a local energy density in the point  $b_0$  (or  $t_0$ ) using the formula

$$E_\xi(a, t_0) = \int E_w(a, b) \xi((b - t_0)/a) db.$$

The window function  $\xi$  acts on interval in vicinity of  $t_0$  and satisfies the relation  $\int \xi(b) db = 1$ . If we take the Dirac function instead of  $\xi$ , then the local energy spectrum has the form

$$E_\delta(a, t_0) = W^2(a, t_0)$$

This characteristics is a very good tool to analyse time dynamics of energy transfer with scales, i. e. energy exchange between process components with different scales in an arbitrary time instant.

Global energy spectrum. A full energy is distributed along the scales, and the global energy spectrum of wavelet transform coefficients reads

$$E_w(a) = \int W^2(a, b) db. \quad (2.8)$$

This is called scalogram or wavelet variance. Describing energy spectrum  $E_w(a)$  via signal energy spectrum in the Fourier domain  $E_f(\omega) = |f^\wedge(\omega)|^2$  we get

$$E_w(a) = \int E_f(\omega) |\psi^\wedge(a\omega)|^2 d\omega, \quad (2.9)$$

and one may observe that wavelet-spectrum of the signal corresponds to the Fourier spectrum of the analysed signal.

Signal energy is defined via energy spectrum by the formula

$$E_f = C_w^{-1} \int E_w(a) da / a^2.$$

Therefore,  $E_f$  is proportional to the surface under the curve  $E_w(a)/a^2$ , and the scalogram exhibits a relative contribution of various scales into full energy, and also exhibits energy distribution of the process along scales.

Since the being analysed function possesses the finite energy, and an analysing wavelet has its mean value equal to zero, the energy spectrum  $E_w(a)$  must tend to zero on both ends of the scales, and it must possess at least one maximum. A location of similar spectrum peaks of the Fourier spectrum  $E_F(\omega)$  usually refers to frequencies and the corresponding modes of a being analysed signal containing a fundamental part of the process energy.

A relation between the scale yielded by the wavelet-transformation and the characteristic scale obtained from Fourier spectrum is shown using the following example. Let  $f(t) = \sin(\omega_0 t) = \sin(2\pi t / T_0)$ . Its wavelet transformation (see formula (7)) reads,

$$W(a, b) = [\exp(i\omega_0 b)\psi^\wedge(a\omega_0) + \exp(-i\omega_0 b)\psi^\wedge(-a\omega_0)]i/2,$$

and spectrum  $E_w(a) = |\psi^\wedge(a\omega_0)|^2$ . A necessary and sufficient condition of a peak occurrence on the scale  $a = a_0$  is that of derivatives  $d\psi^\wedge(a\omega_0)/da = 0$  for  $a = a_0$ . This condition is satisfied for  $a_0\omega_0 = \omega_\psi$ , where  $\omega_\psi$  is the constant depending on the wavelet  $\psi$  of a frequency dimension. For many wavelets the constant  $\omega_\psi$  may be found in an analytic way: for HAAR and MHAT wavelets it is equal to  $1,484\pi$  and  $2^{1/2}$ , respectively.

On the other hand, if the scalogram has a peak for  $a = a_0$ , the characteristic time scale is defined by  $d = \frac{T_0}{2} = \frac{a_0\pi}{\omega_\psi}$ . The  $1/2$  coefficient appears because a scale of an elementary characteristic term is presented. In this interpretation, sinus has two such terms.

Note that  $\omega_\psi$  can be only obtained for a relatively simple function. Extending the result to an arbitrary signal (non-harmonic), we assume that the maximum  $E_w(a)$  location can be interpreted as average extension of an elementary term, introducing the fundamental contributions into energy of the analysed process. This behaviour holds for many known signals with various wavelets and can be treated as a very good approximation (see, for instance, reference [48]).

### 3. Parametric Vibrations of Flexible Rectangular Plates.

**3.1. Problem formulation and solution algorithm.** The problem of computations of parametric vibrations of flexible plates from a point of view of qualitative theory of differential equations is rather rarely investigated. The known T. von Kármán equations are cast in the form [51]:

$$\frac{\partial^2 w}{\partial t^2} + \varepsilon \frac{\partial w}{\partial t} = -\frac{1}{12(1-\nu^2)} \Delta^2 w + L(w, F) - \Delta_p w + q, \quad (3.1)$$

$$\Delta^2 F = -\frac{1}{2} L(w, w).$$

The system (2.1) is reduced to non-dimensional form in the following way

$$x = a\bar{x}, \quad y = b\bar{y}, \quad w = 2H\bar{w}, \quad \lambda = a/b, \quad t = t_0\bar{t}, \quad \varepsilon = (2H)\bar{\varepsilon},$$

$$P_x = \frac{E(2H)^3}{b^2} \bar{P}_x, \quad P_y = \frac{E(2H)^3}{a^2} \bar{P}_y, \quad q = \frac{E(2H)^4}{a^2 b^2} \bar{q}.$$

The following notation is used:  $q(x, y, t)$  is the function of the transversal load;  $P_x(y, t)$ ,  $P_y(x, t)$  are the functions of longitudinal loads along the axes  $Ox$  and  $Oy$ , respectively;  $2H$  is the plate thickness;  $a, b$  are the plate dimensions;  $\varepsilon$  is the damping coefficient;  $E$  is Young modulus;  $\nu$  is Poisson's coefficient;  $w(x, y, t)$  and  $F(x, y, t)$  are

deflection and Airy's function, respectively. The coordinates origin is located in left down angle. The  $Ox$  and  $Oy$  axes coincide with the plate edges, and  $z$  axis goes into the Earth centre;  $(x, y) \in \bar{G} = \{0 \leq x \leq 1; 0 \leq y \leq 1\}$ ,  $0 \leq t \leq t_{end}$ . The operators  $L(w, F)$ ,  $\Delta(\cdot)$ ,  $\Delta_p(\cdot)$  have the form

$$L(w, F) = \frac{\partial^2 w}{\partial x^2} \frac{\partial^2 F}{\partial y^2} - 2 \frac{\partial^2 w}{\partial x \partial y} \frac{\partial^2 F}{\partial x \partial y} + \frac{\partial^2 w}{\partial y^2} \frac{\partial^2 F}{\partial x^2},$$

$$\Delta(\cdot) = \frac{\partial^2(\cdot)}{\partial x^2} + \frac{\partial^2(\cdot)}{\partial y^2}, \quad \Delta_p(\cdot) = P_x \frac{\partial^2(\cdot)}{\partial x^2} + P_y \frac{\partial^2(\cdot)}{\partial y^2}.$$

The squared plates ( $\lambda = 1$ ) are further analysed, and the following initial conditions are used

$$w|_{t=0} = \varphi_1(x, y), \quad w|_{t=0} = \varphi_2(x, y). \quad (3.2)$$

For the space the boundary conditions are applied

$$w = w_{xx} = F = F_{xx} = 0, \quad (x = 0; 1), \quad x \leftrightarrow y, \quad (3.3)$$

which correspond to the ball support on the flexible non-stretched in the tangent plane ribs.

Although the prepared algorithm allows for investigation of various boundary conditions, only (3.3) are used in this paper.

The partial differential equations (3.1) - (3.3) are reduced to the system of ordinary differential equations using a difference method  $O(h^2)$ .

The partial derivatives with respect to  $x$  and  $y$  in system (3.1) are approximated by difference relations with the error of  $O(h^2)$ , applying development into Taylor series in the vicinity of the point  $(x_i, y_i)$  and using powers of  $h$  being the step of the following mesh

$$\bar{G}_n = \{0 \leq x_i; y_i \leq 1, x_i = ih, i, j = \overline{0, N}, h = 1/N\}.$$

The difference relations for partial derivatives of second and fourth orders are obtained, which are next used to obtain the system of ordinary differential equations in time and the system of algebraic equations with respect to  $F_{ij}$ :

$$\frac{\partial^2 w_{ij}}{\partial t^2} + \varepsilon \frac{\partial w_{ij}}{\partial t} = \{A(w_{ij}) + B(w_{ij}, F_{ij})\} + q_{ij}, \quad (3.4)$$

$$D(F_{ij}) = E(w_{ij}).$$

The difference operators  $A_2(w_{ij})$ ,  $B_2(w_{ij}, F_{ij})$ ,  $D_2(F_{ij})$ ,  $E_2(w_{ij})$  occurring in (3.4) have the following form

$$A(w_{ij}) = \frac{1}{12(1-\nu^2)} \left( \lambda^{-2} \Lambda_{x^4} w_{ij} + 2 \Lambda_{x^2} \Lambda_{y^2} w_{ij} + \lambda^2 \Lambda_{y^4} w_{ij} \right),$$

$$A(w_{ij}, F_{ij}) = \Lambda_{x^2} w_{ij} (\Lambda_{y^2} F_{ij} - P_x) + \Lambda_{y^2} w_{ij} (\Lambda_{x^2} F_{ij} - P_y) - 2 \Lambda_{x^2 y^2} w_{ij} \Lambda_{x^2 y^2} F_{ij},$$

$$D(F_{ij}) = 12(1-\nu^2) A(F_{ij}),$$

$$E(w_{ij}) = \Lambda_{x^2} w_{ij} \Lambda_{y^2} F_{ij} + [\Lambda_{xy} w_{ij}]^2,$$

where:  $\Lambda_{x^k y^k}$  ( $k = 0, 2, 4$ ) are known difference operators of the corresponding derivatives.

The obtained system of non-linear differential-difference equations with respect to  $w_{ij}$  has the following vector form

$$\frac{dw}{dt} = Q(W, F, t), \quad AF = P, \quad (3.5)$$

where  $W$  is the being sought vector with components  $(w_{ij})$ ,  $A$  is the matrix,  $F$  is the being sought vector with components  $F_{ij}$ ,  $P$  is the vector of right hand side of the second equation of (3.5) depending on  $w_{ij}$ .

**3.2. Application of wavelet analysis to investigate complex parametric vibrations of flexible plates.** A stability of isotropic ( $\nu = 0,3$ ) squared ( $\lambda = 1$ ) plate subjected to a longitudinal load  $P_x = P_x^0 \sin \omega t$ ,  $\omega = 8$ ,  $\varepsilon = 1$  is investigated. The following initial conditions are applied

$$w|_{t=0} = A \sin \pi x \sin \pi y (A = 1 \cdot 10^{-3}) \quad \dot{w}|_{t=0} = 0.$$

In this report a transition to chaos using the control parameter  $\{P_x^0\}$  is analysed. The investigation is carried out using only one boundary conditions type, i. e.

$$w|_{\Gamma} = w_n|_{\Gamma} = F|_{\Gamma} = F_n|_{\Gamma} = 0,$$

where  $\Gamma$  is the border of the space  $G = \{x, y | 0 \leq x \leq 1; 0 \leq y \leq 1\}$  and  $n$  denotes a normal to the  $G$  border. In the Figs. 4, 5 the graphs  $P^0[w_{\max}(0,5;0,t)]$  corresponding to either  $P_x = P^0 \sin \omega t$  (Fig. 4) or  $P_x = P_y = P^0 \sin \omega t$  (Fig. 5) longitudinal loads are shown. In both cases reported the same frequency  $\omega = 8$  is taken.

On the vertical axes two scales are used: the values of the parameter  $P^0$  and the numbered qualitatively different spaces characterizing system dynamics. The found vibration types and the corresponding numbers are included in Table.

An investigation of complex vibrations required a construction (for each point  $(ij)$  of the mesh  $\bar{G}_n$ ) of the time histories  $w_{ij}(t)$ ,  $\dot{w}_{ij}(t)$ , phase portraits  $\dot{w}_{ij}(w_{ij})$ , Poincaré sections  $w_{ij}^T(w_{ij}^{(t+T)})$  (where  $T$  denotes period of a longitudinal load), power spectrum  $\lg s(w)$  and an application of wavelet analysis. The so-called Morlet-wavelet function is used, which represents a harmonic wave. Contrary to a standard Fourier analysis, where only frequency ( $\omega$ ) dependent analysis yields also time localization of the traced process,

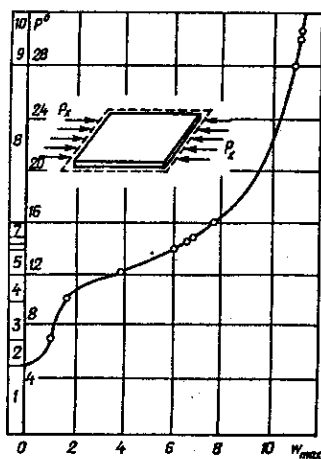


Fig. 4

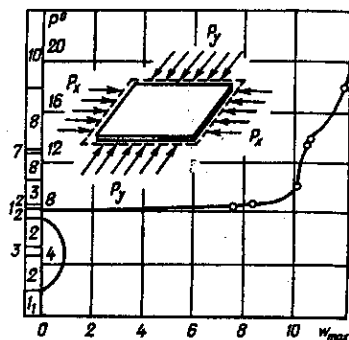


Fig. 5



Space number	Vibration types
1, $l_1, l_2$	fixed point
2	periodic vibrations
3	Andronov-Hopf bifurcation
4	quasiperiodic vibrations
5	crisis
6	post-crisis
7	regular vibrations with a new frequency
8	quasiperiodic vibrations with new frequencies
9	intermittency
10	chaos

the spectrum  $W(a, b) = A(w, t)$  is constructed in the form of surfaces for each  $P^0$  value. In addition, further important informations are carried out by the projections into plane  $(t, w)$  with iso-curves (iso-levels) and gray-scale representations of the evolution of local extremum curves. Besides, the cross sections for  $t = 50$  of three dimensional spaces are reported together with included FFT (Fast Fourier Transforms). The extremely large amount of computations implies that the above mentioned characteristics are similar for all points  $(ij)$  of the mesh  $\bar{G}_n$  partition. Therefore, for some characteristics only the results for the plate centre are shown ( $i = j = 0,5$ ). In Figs. 6 - 8 the computational results for the amplitude of exciting harmonic force  $P^0 = 5; 10; 12; 14; 14,7; 15,1; 18; 28; 30$  for one sided stretching are reported. In Figs. 9 - 12 similar like computation results for two sided stretching are shown for  $P^0 = 2,5; 3; 5; 7; 7,25; 8,25; 8,5; 9; 12; 13; 14; 19$ . In each figure blocks of three groups of six windows are shown, and the signal  $W(t)$  begins each of the group (see the attached  $P^0$  value shown in the right higher window corner).

For  $P^0 = 5$  all six characteristics describe periodic vibrations with the excitation frequency, which is clearly visible on both FFT and wavelet-analysis. For  $P^0 = 10$  in  $A(w, t)$  newly born frequencies are observed, which evaluate with time (see isoclines in plane  $(t, w)$  and in gray-shadow picture  $(t, w)$ ). Note that by FFT only the fundamental frequency is caught. For  $P^0 = 12$  the deflections increased more than two times, and the fundamental frequency increased two time (period doubling (Hopf) bifurcation). Further increase of  $P^0$  leads to strange attractor ( $SA_1$ ) occurrence, which is reported for  $P^0 = 12$ . The frequencies essentially depend on time. A further slight increase of the forcing amplitude (see  $P^0 = 14$ ) results in a crisis. This conclusion is derived on observation of all characteristics. The deflections increased almost two times, and they behave in chaotic manner (see also the phase portrait). All of the frequencies change with time and there does not exist any relations between them, but there are time instants where the series of Hopf bifurcation occurs. Further increase of the parameter  $P^0$  [ $P^0 = 14,7; 15,1$ ] causes a qualitative change of plates vibrations although the vibrations amplitude does not undergo any changes. Another type of a strange attractor ( $SA_2$ ) appears on the phase plane. Further increase of  $P^0$  (see Figs. corresponding to  $P^0 = 18$ ) only slightly changes vibrations character, but then intermittency chaos is observed (see  $P^0 = 28$ ). In chaotic responses the periodic windows are observed within time intervals  $50 \leq t \leq 70$  (see all characteristics associated with  $P^0 = 28$ ). Further increase of  $P^0$  (see  $P^0 = 30$ ) leads to full chaos occurrence. Wavelet analysis tools (see  $A(w, t)$  and  $(t, w)$ , and grey-shadowing pictures) exhibit full irregularity, and frequencies depend on time.

In general, the characteristics flexible plate vibrations features subjected to two sided periodic excitations are similar to that of one sided periodic excitation.

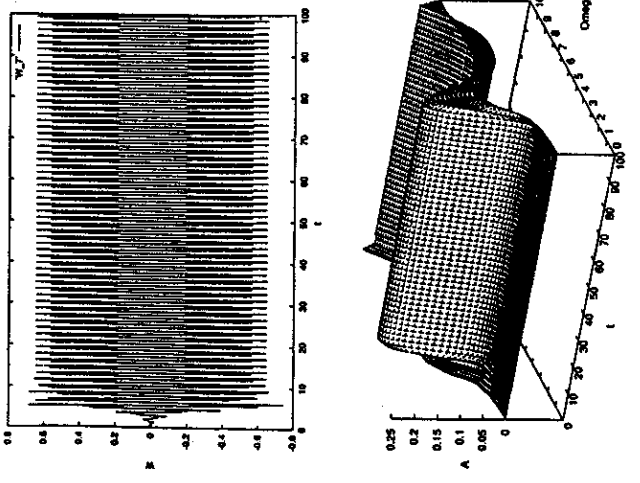
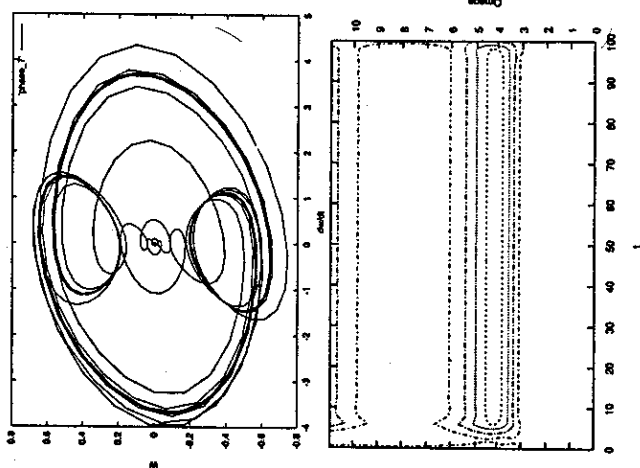
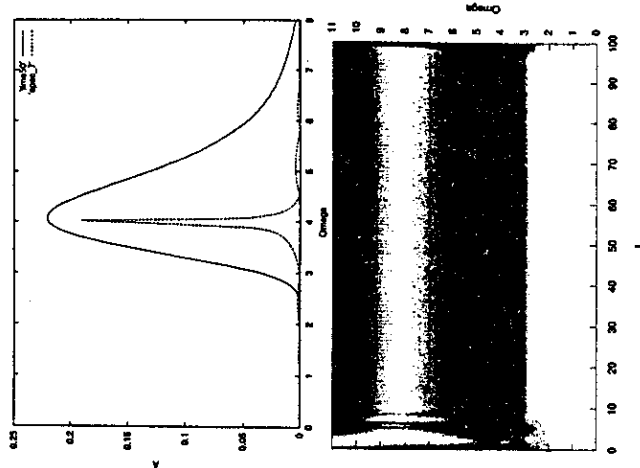
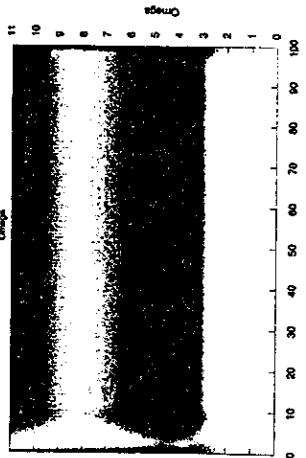
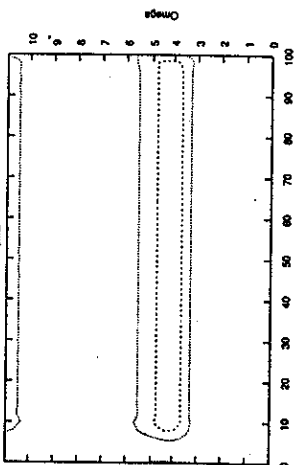
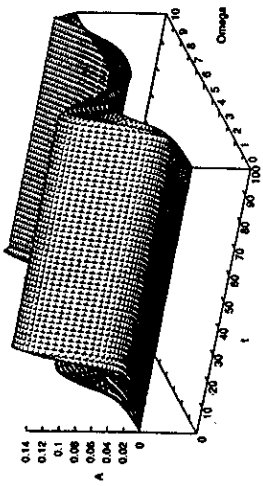
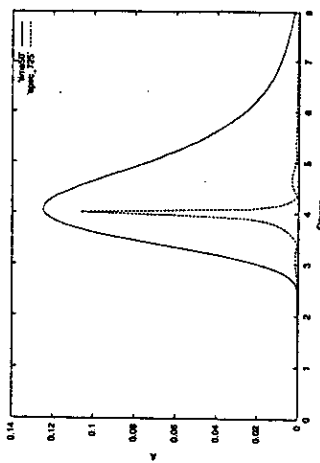
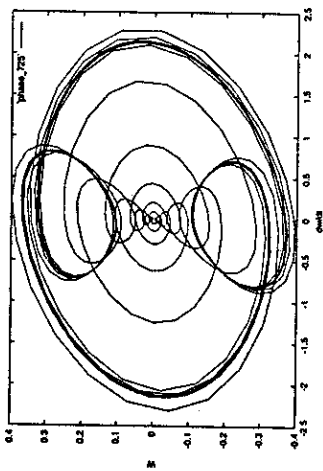
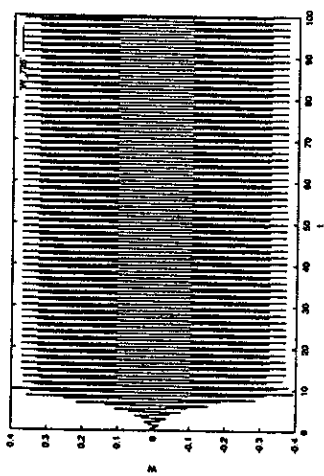
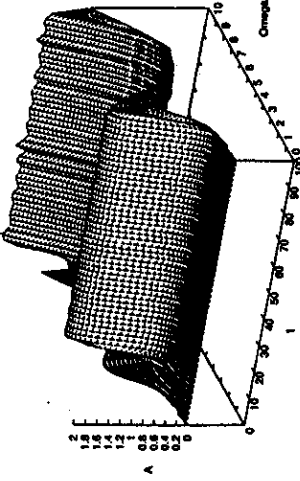
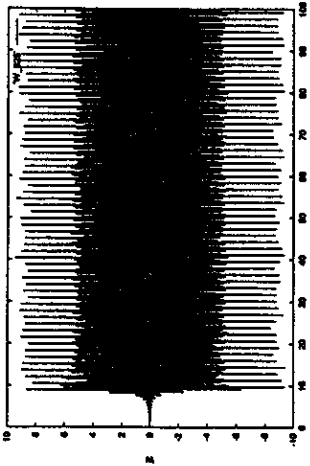
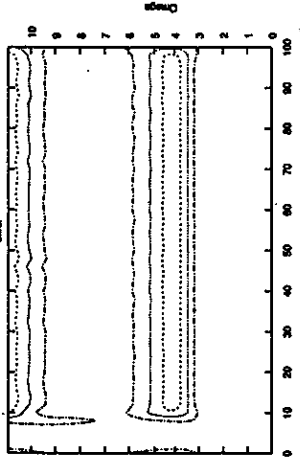
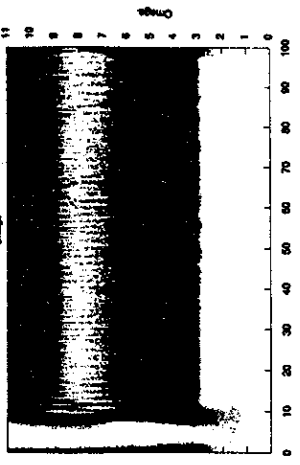
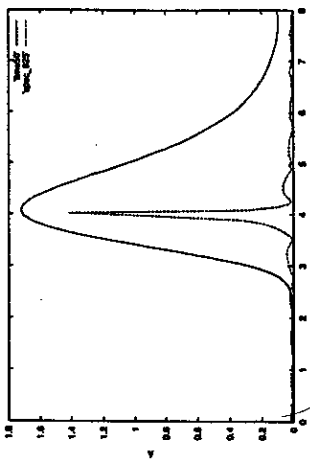


Рис. 6



Продолжение рис. 6



Продолжение рис. 6

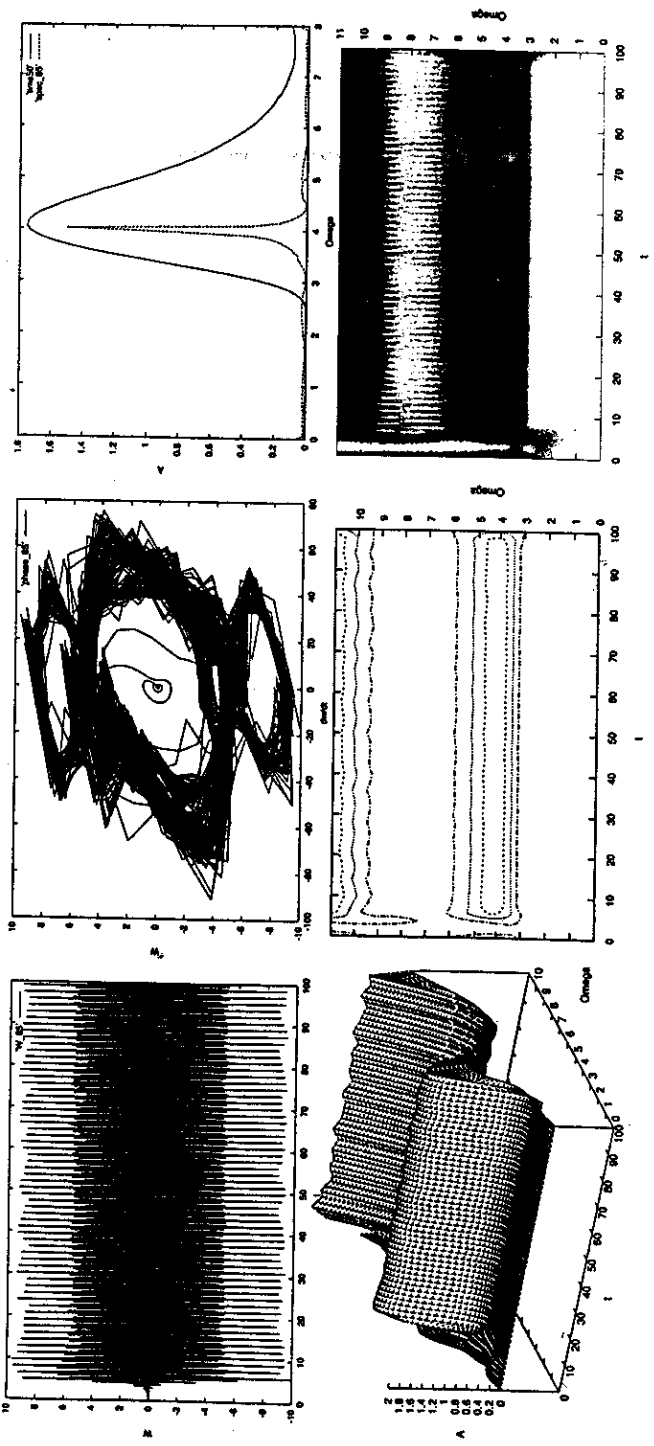
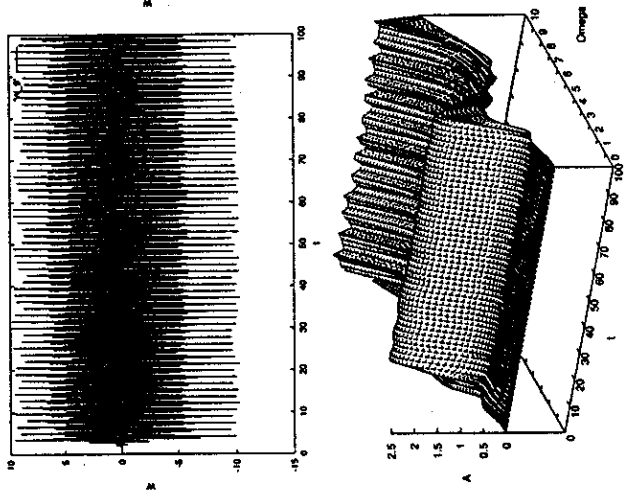
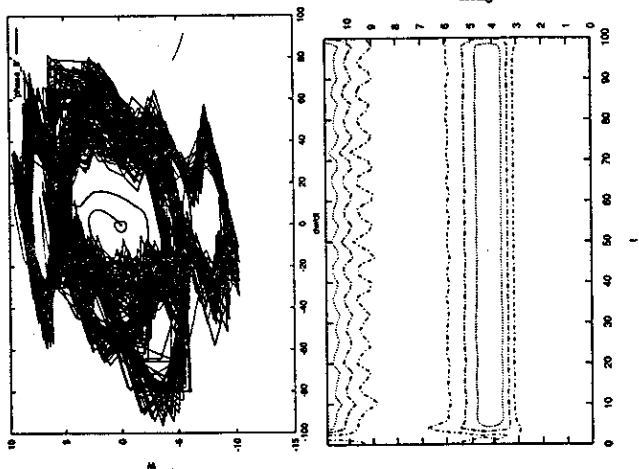
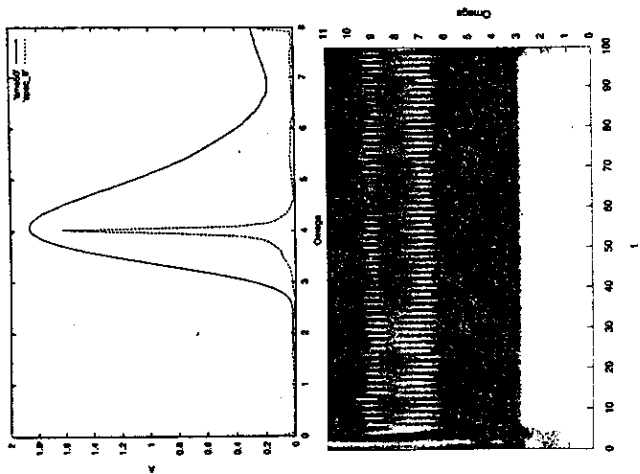
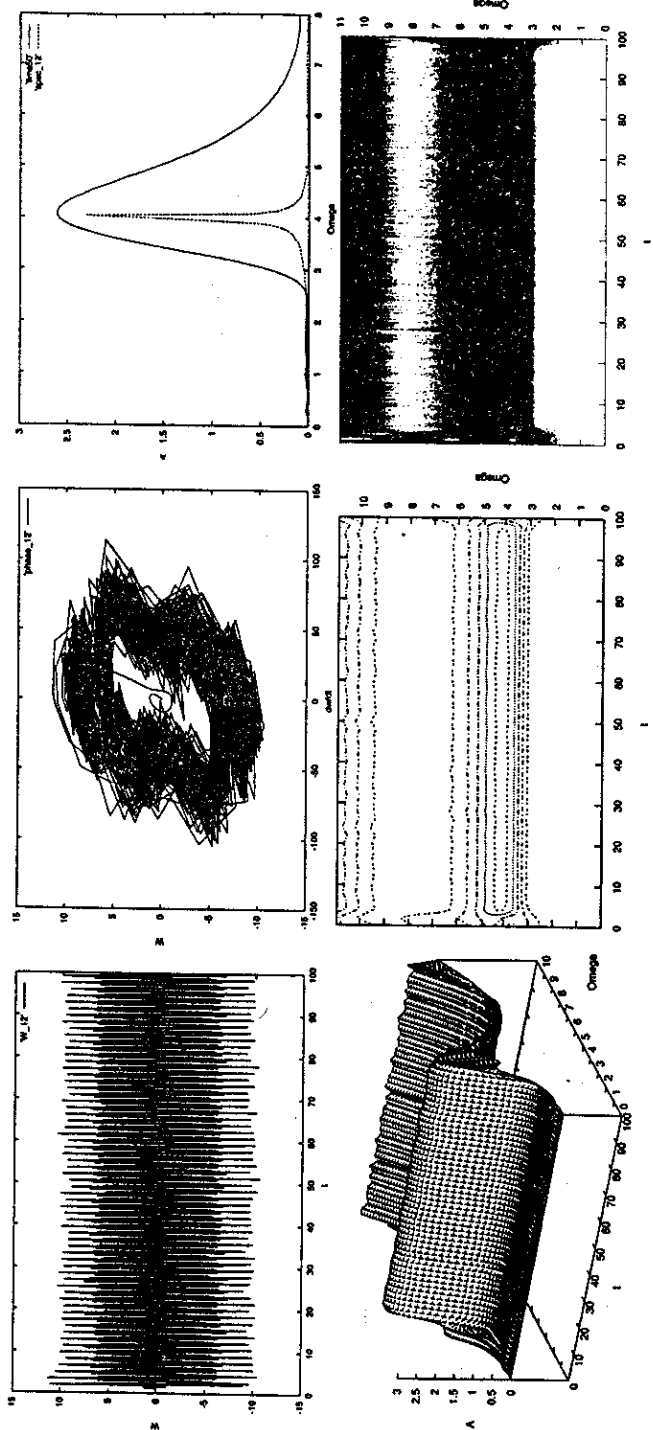


Рис. 7



Продолжение рис. 7



Продолжение рис. 7

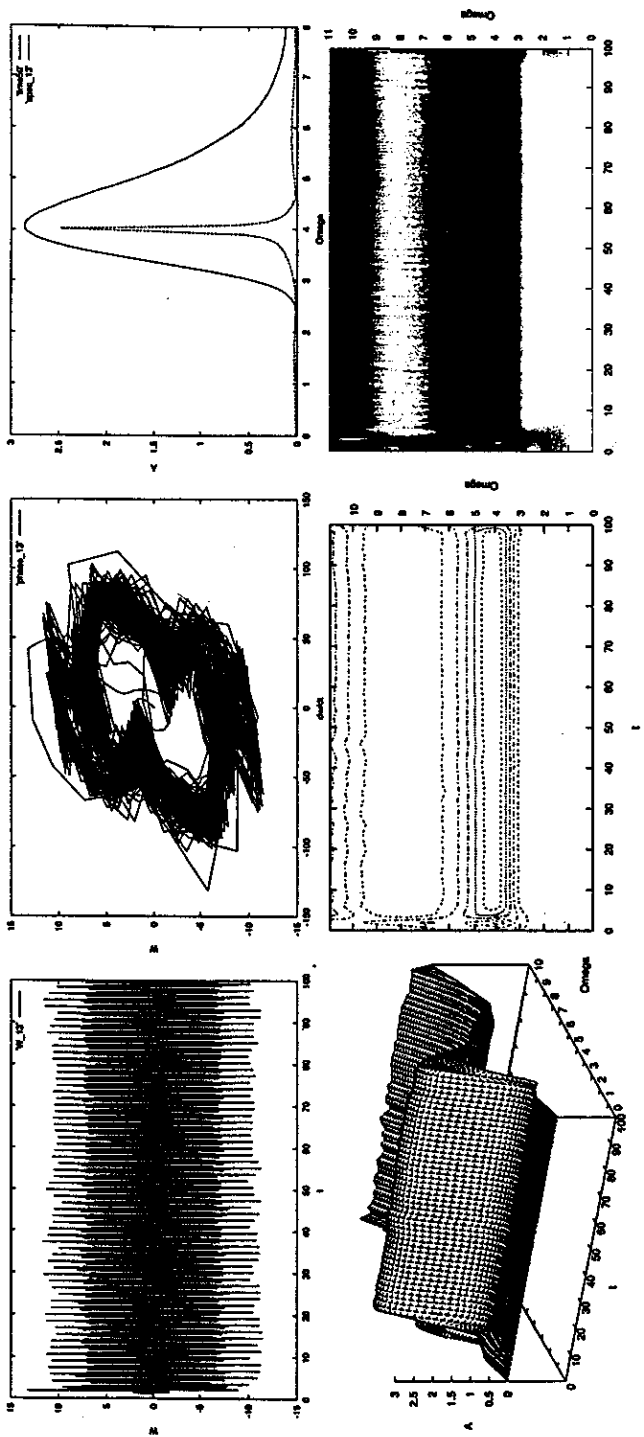
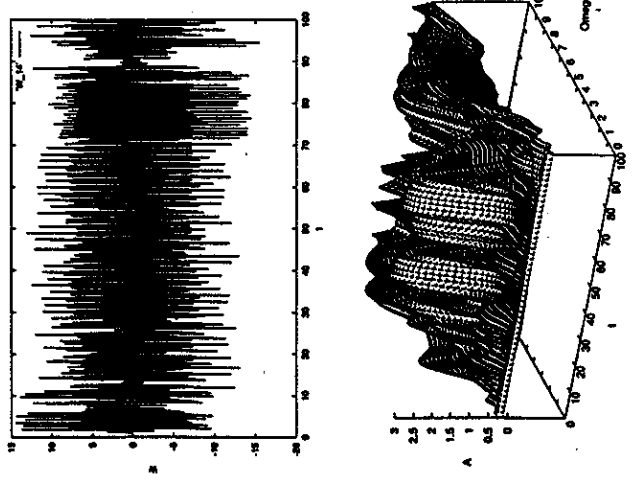
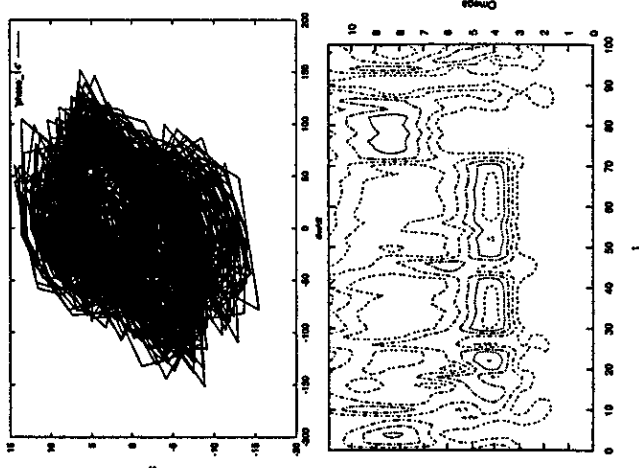
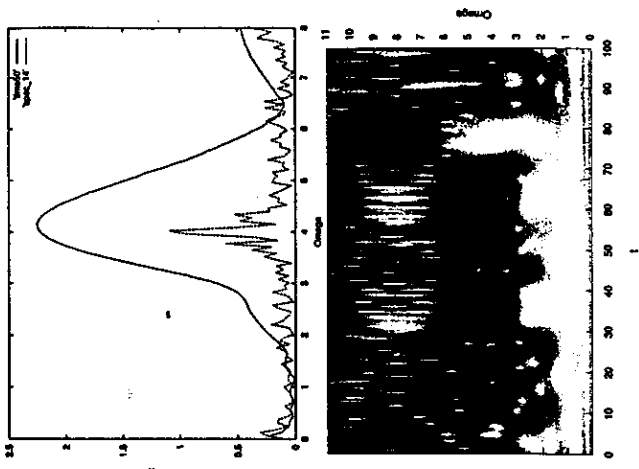
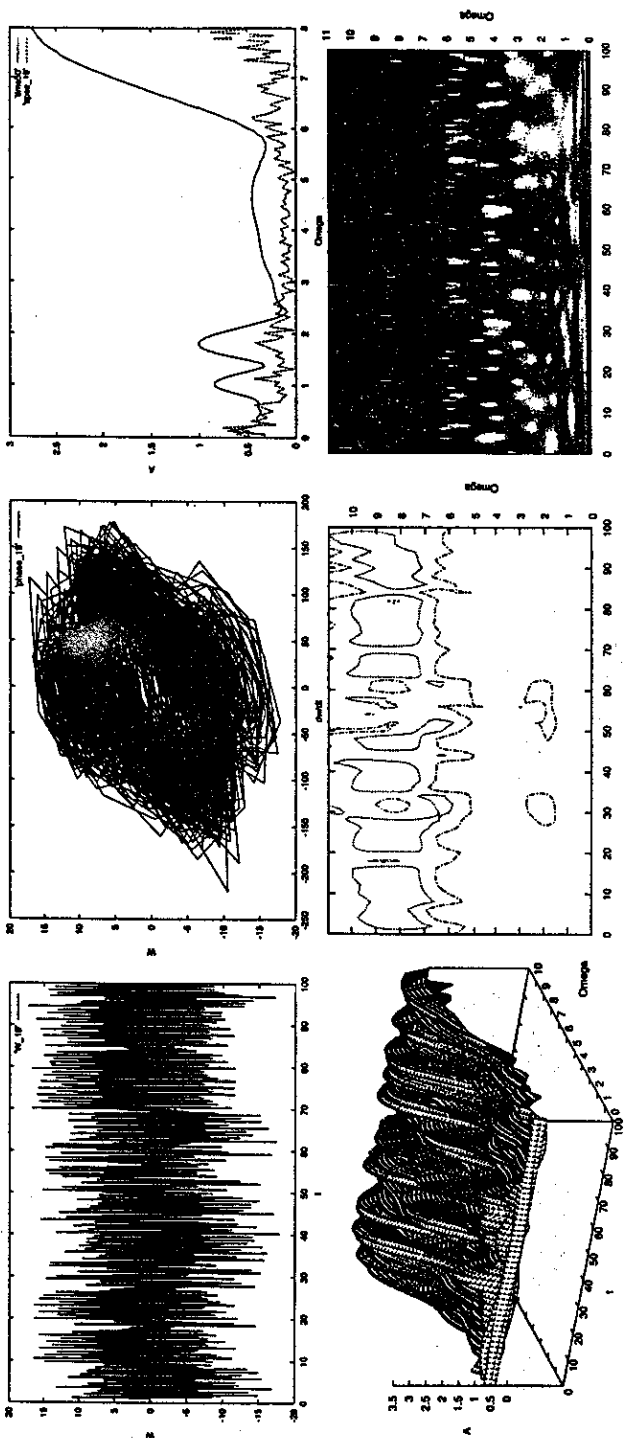


Fig. 8





Продолжение рис. 8



Продолжение рис. 8

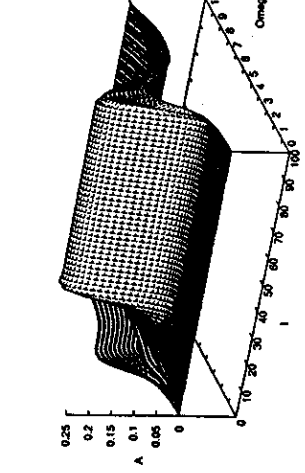
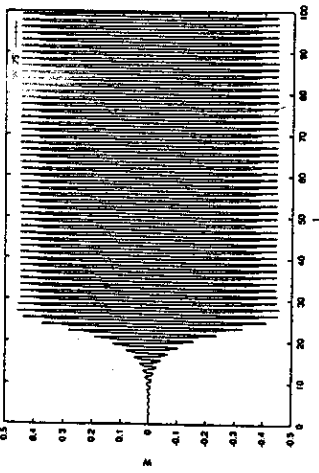
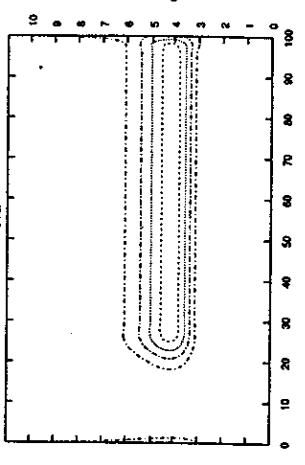
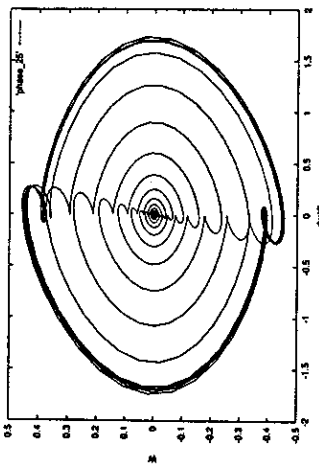
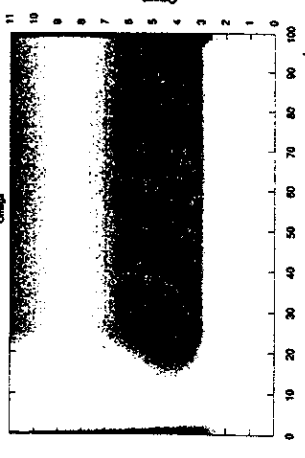
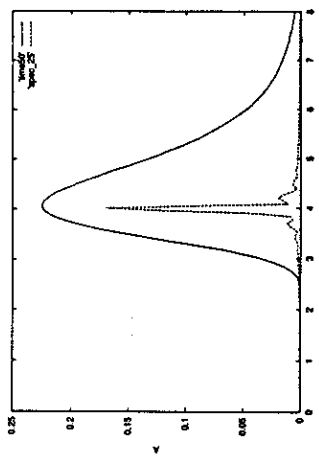
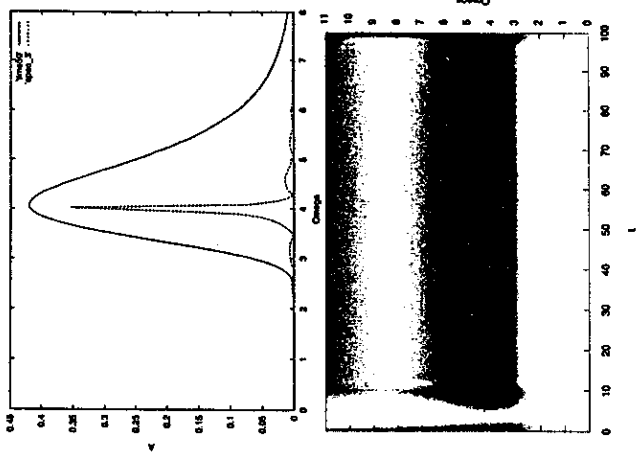
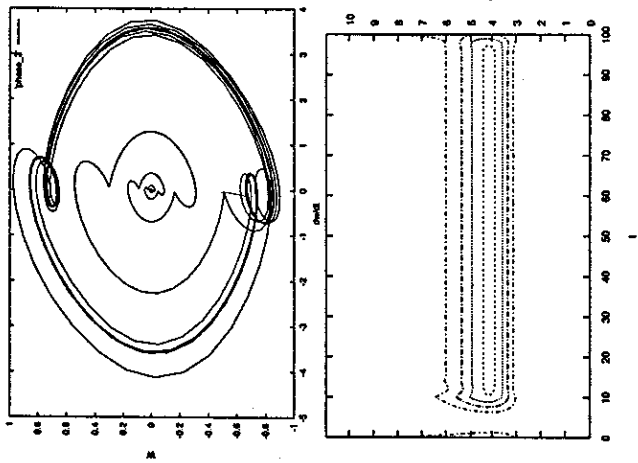
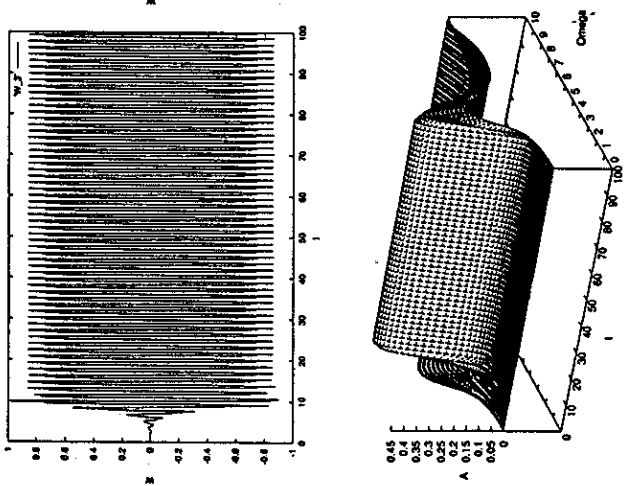
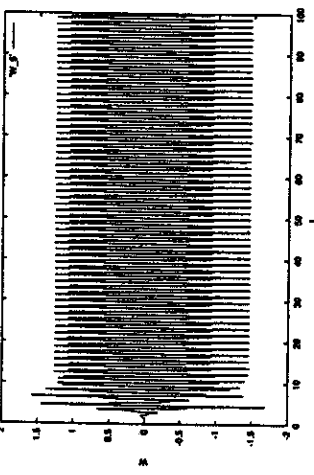
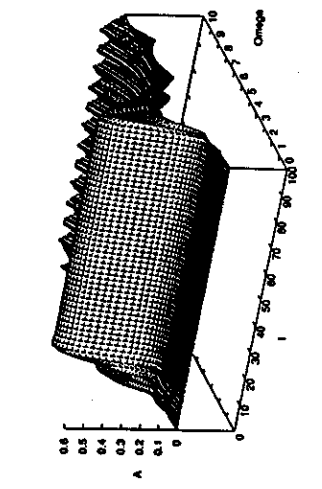
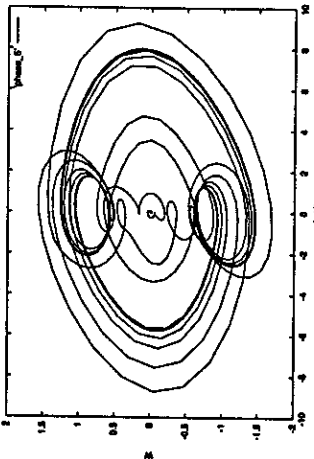
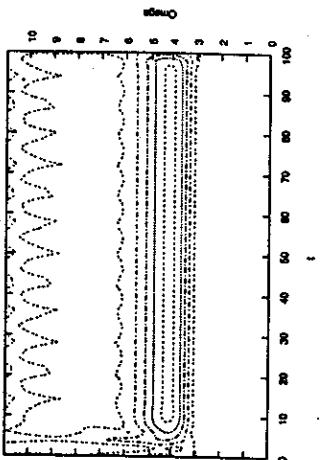
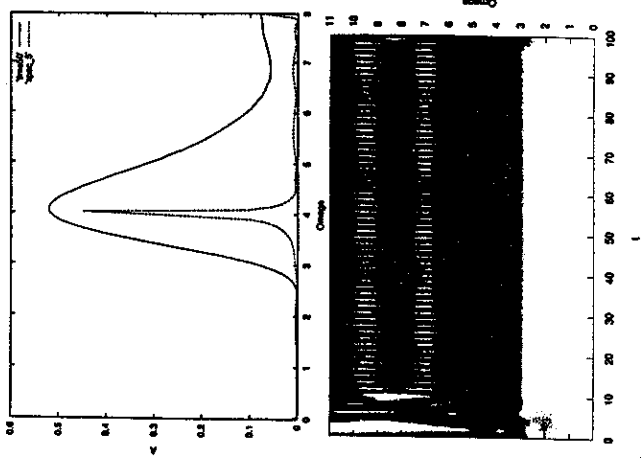


Рис. 9



Продолжение рис. 9



Продолжение рис. 9

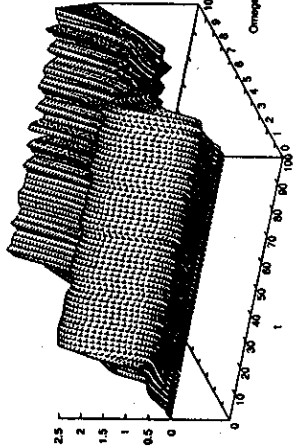
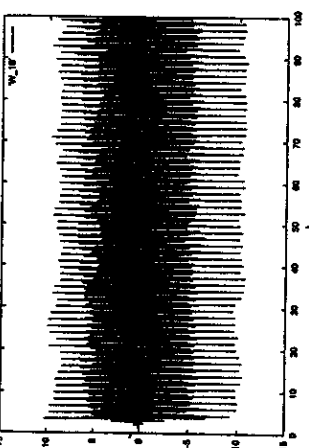
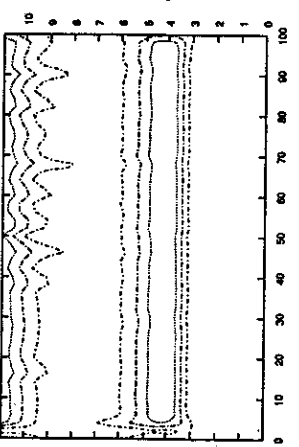
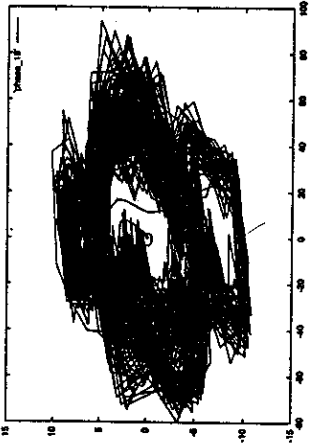
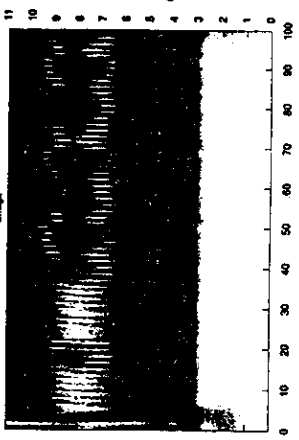
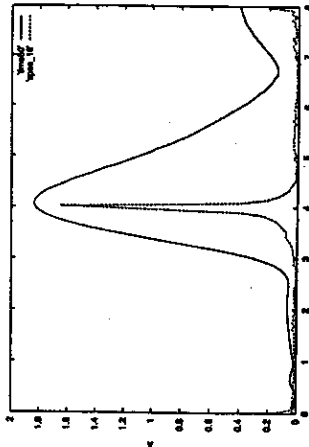
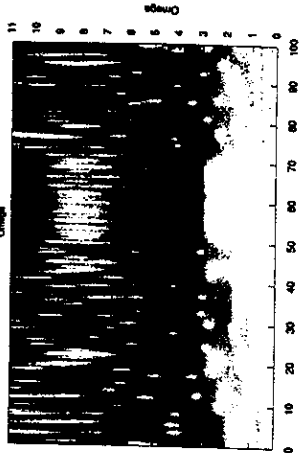
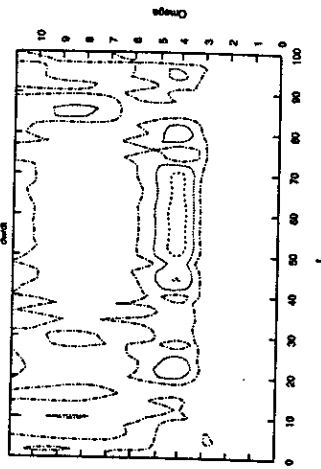
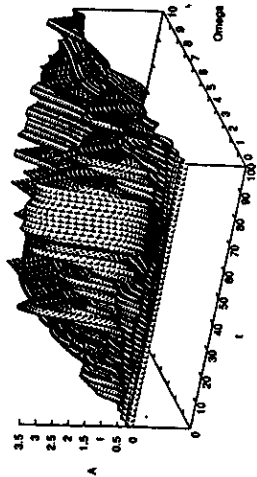
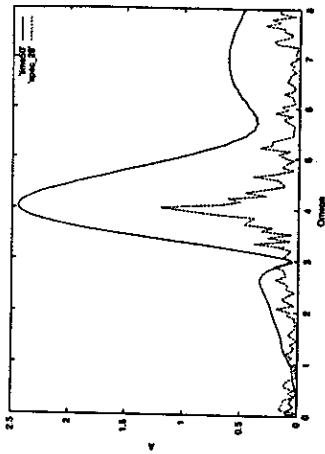
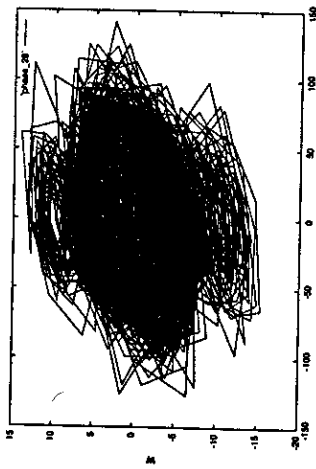
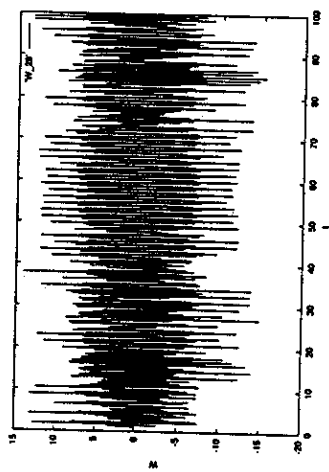
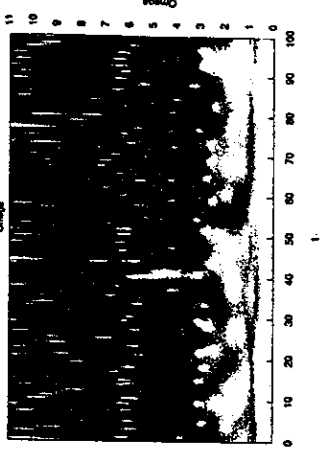
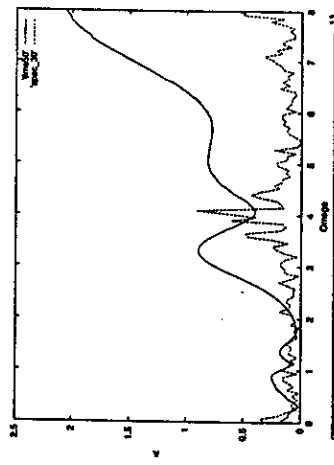
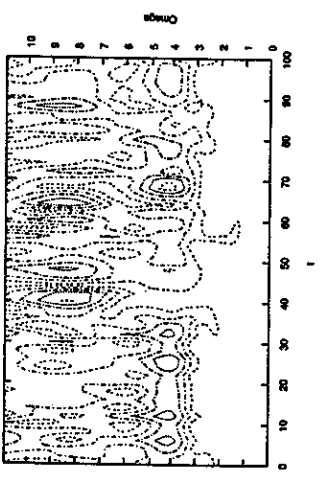
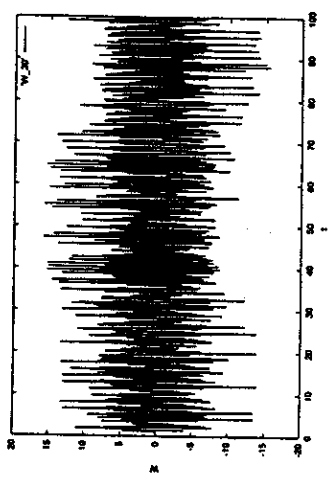


Рис. 10

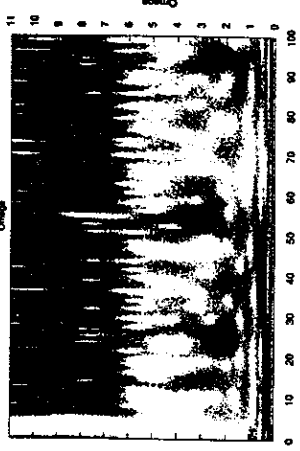
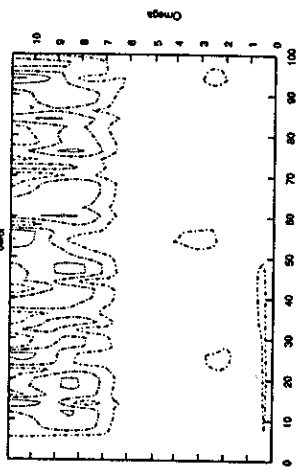
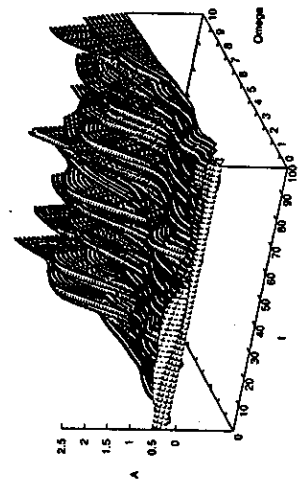
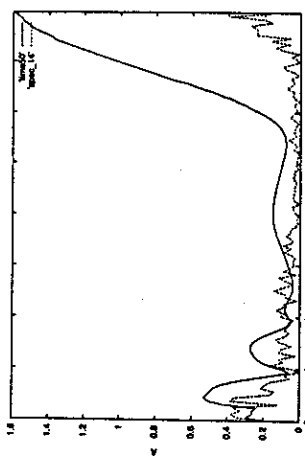
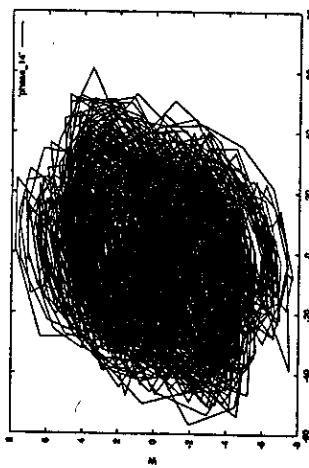
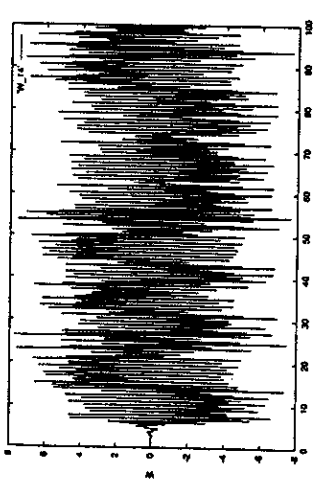


Продолжение рис. 10

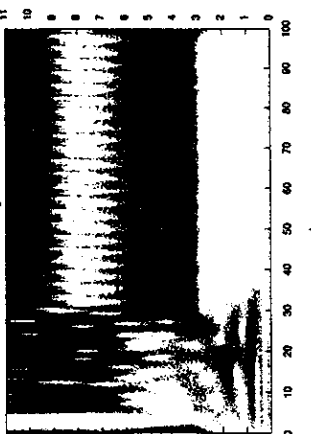
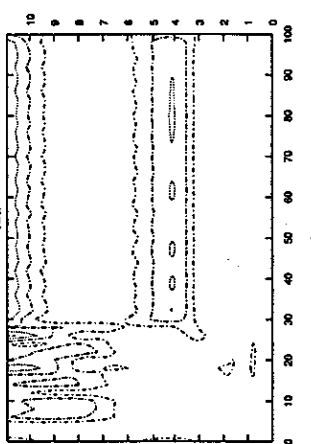
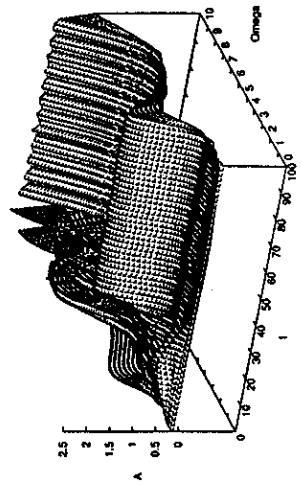
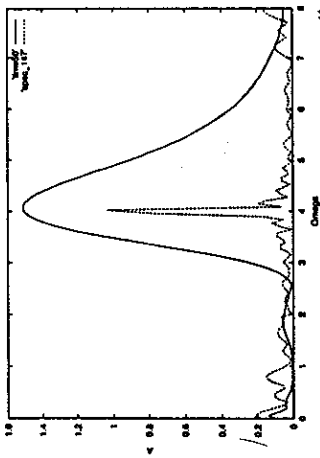
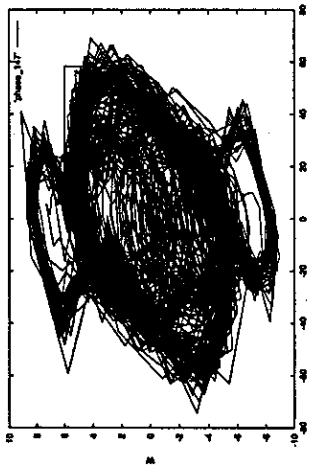
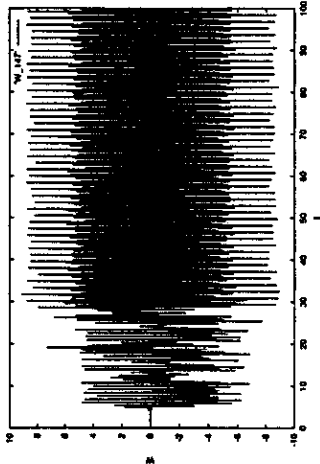


Продолжение рис. 10

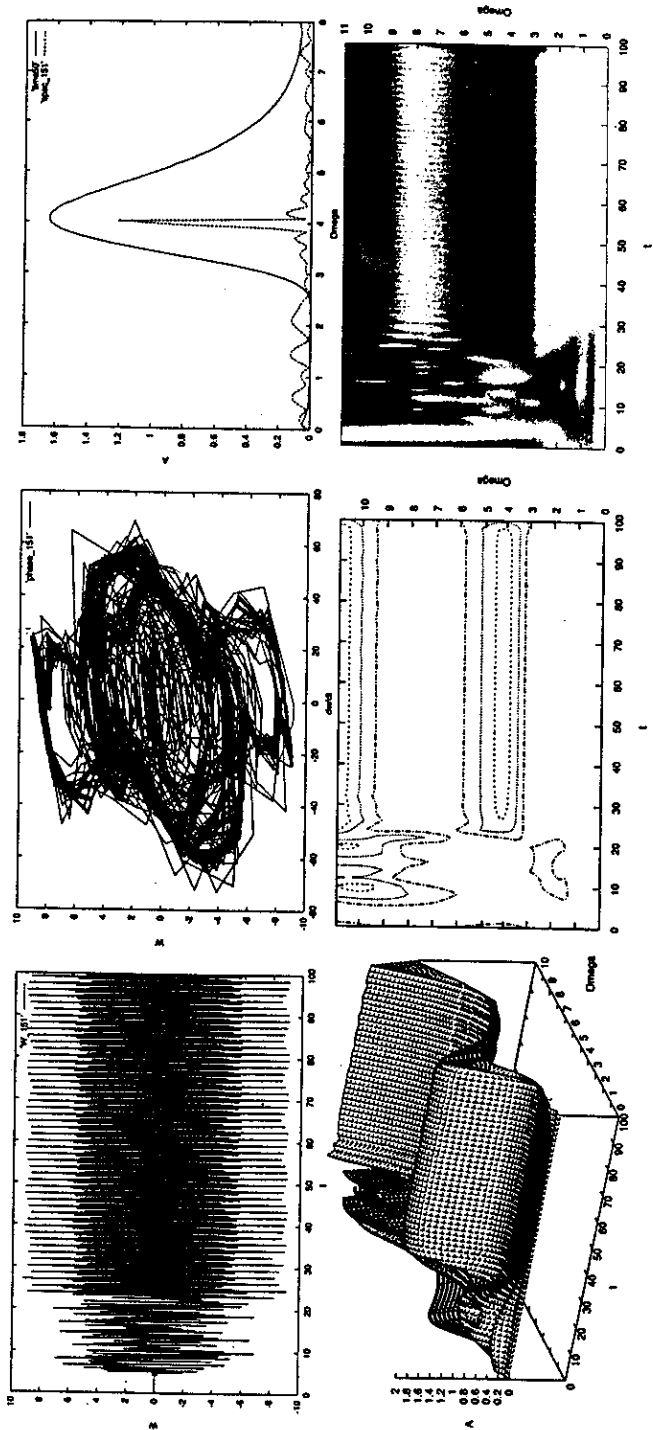




*Puc. 11*



Продолжение рис. 11



Продолжение рис. 11

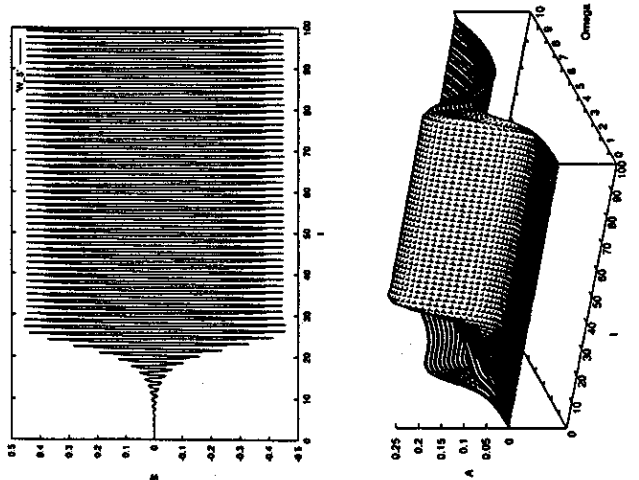
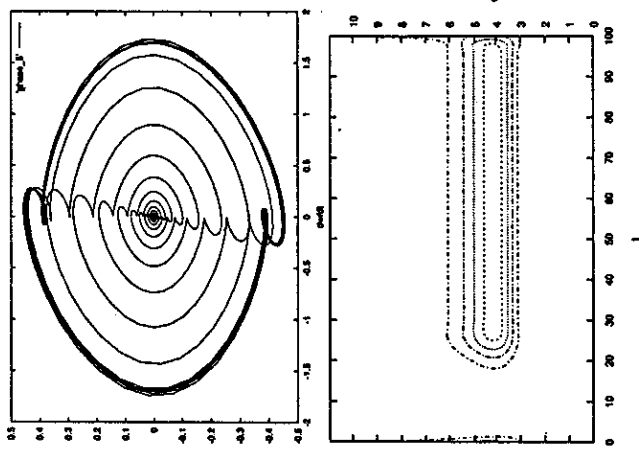
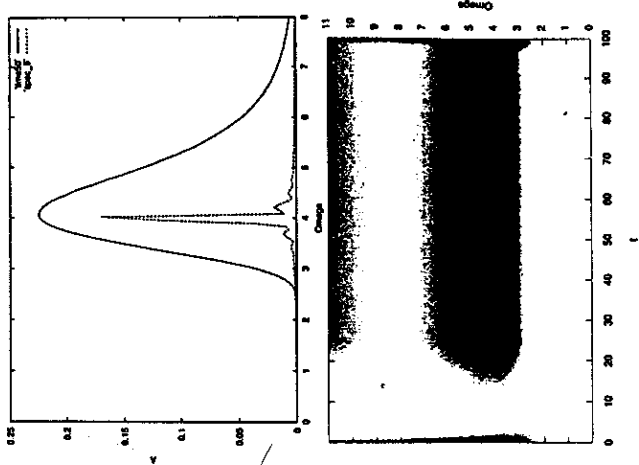
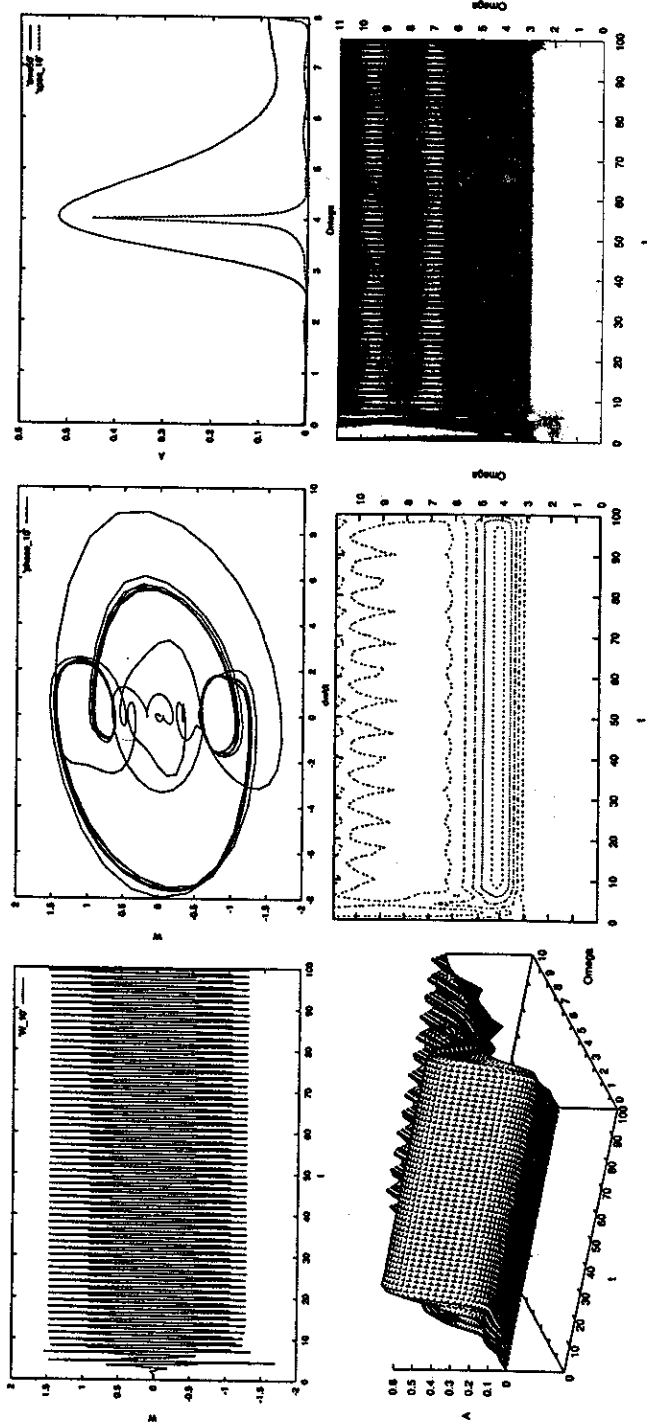
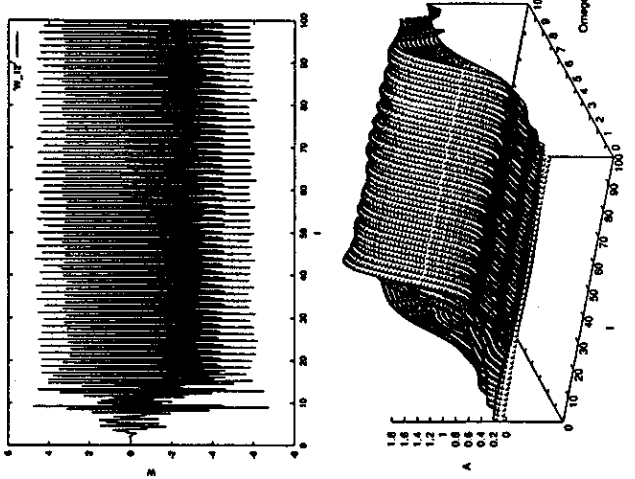
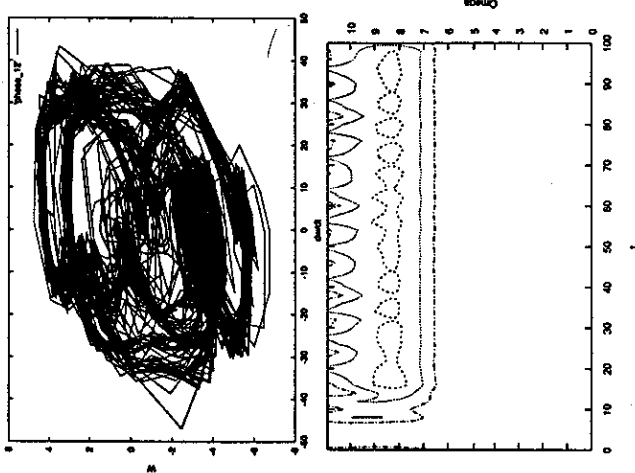
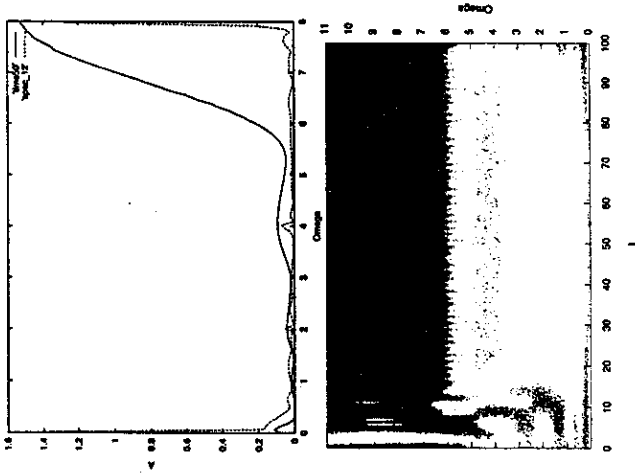


Fig. 12



Продолжение рис. 12



Продолжение рис. 12

**4. Concluding Remarks.** First, both a background and an overview of wavelet-based approach are outlined. Second, Fourier transform and Fourier series analysis versus wavelet-based methods is illustrated and discussed. A special attention is paid to wavelet method advantages owing to frequency-time localization. Basic functions of wavelet transformation are overviewed. Properties and application of the wavelet transformation are rigorously discussed. In the second part of this paper, i.e. section 3, parametric regular and chaotic vibrations, as well as various bifurcations, exhibited by flexible rectangular plates are analysed. The von Kármán partial differential equations are transformed to a set of ordinary differential and algebraic equations, which is further analysed using the wavelet-based technique. Among others, it is shown that the applied Morlet-wavelet function representing a harmonic wave yields a larger information amount in comparison to a standard FFT approach.

Two main concluding remarks with respect to flexible plate dynamics follow:

1. Fourier-analysis and wavelet-analysis overlap only in the case of simple type of longitudinally and sinusoidally driven plate vibrations.

2. Wavelet-analysis seems to be a very good tool for detailed investigation of spatial structure dynamics (here a plate) including all remarkable feature of regular (periodic and quasi-periodic), and chaotic dynamics, as well as bifurcation, crises and intermittent states.

**Р Е З Ю М Е .** Дано огляд методів, основаних на вейвлетях, і окреслено їх переваги в порівнянні зі стандартними підходами. Далі подібний до вейвлетного аналіз застосовано для дослідження параметричних коливань гнучких пластин, на які діє синусоїдальне навантаження. Зокрема, проаналізовано сценарій переходу від регулярного руху до хаосу.

**S U M M A R Y.** Wavelets-based methods are reviewed, and their advantages in comparison to standard approaches are outlined. Then, a wavelet-like analysis is applied to investigate parametric vibrations of flexible plates sinusoidally loaded. In particular, a scenario leading from regular motion to chaos is analysed.

**Key words:** flexible plates, parametric vibrations, regular motion, chaos, wavelets-based methods.

1. J. Morlet and A. Grossmann, "Decomposition of Hardy functions into square integrable wavelets of constant shape", *SIAM J. Math. Anal.*, 15(4), 723 – 736 (1984).
2. L.A. Wong and J. C. Chen, "Nonlinear and chaotic behavior of structural system investigated by wavelet transform techniques", *Int. J. Nonl. Mech.*, 36(2), 221 – 235 (2001).
3. M. A. Alves, P. Cruz, A. Mendes, F. D. Magalhães, F. T. Pinho, P. J. Oliveira, "Adaptive multiresolution approach for solution of hyperbolic PDEs", *Comp. Meth. Appl. Mech and Eng.*, 2904 (2002).
4. P. Yiou, D. Sornette, M. Ghil, "Data-adaptive wavelets and multi-scale singular-spectrum analysis" *Physica D*, 142(3 – 4), 254 – 290 (2000).
5. R. Kronland-Martinet, J. Morlet, A. Gossmann, "Analysis of sound patterns through wavelet transforms", *Int. J. of Pattern Recognition and Artificial Intelligence*, 1(2), 273 – 302 (1987).
6. J. Fröhlich and K. Schneider, "Computation of decaying turbulence in an adaptive wavelet basis", *Physica D*, 134(3), 337 – 361 (1999).
7. A. K. Alekseev and M. Navon, "The analysis of an ill-posed problem using multi-scale resolution and second-order adjoint techniques", *Comp. Meth. Appl. Mech and Eng.*, 190(15 – 17), 1937 – 1953 (2001).
8. J. Liandrati and Ph. Tchamitchian, "Resolution of the 1D regularized Burgers equation using a spatial wavelet approximation", *Institute for Computer Applications in Science and Engineering Report No. 90 – 83*, Universities Space Research Association (1990).
9. S. Guan, C.-H. Lai, G. W. Wei, "A wavelet method for the characterization of spatiotemporal patterns", *Physica D*, 163(1 – 2), 49 – 79 (2002).
10. H. Nakao, T. Mishihiro, M. Yamada, "Visualisation of correlation cascade in spatialtemporal chaos using wavelets", *Int. J. Bifur. Chaos*, 11(5), 1483 – 1493 (2001).
11. R. W. Wittenberg and P. Holmes, "Spatially localized models of extended systems", *Nonl. Dynamics*, 25, 111 – 132 (2001).
12. W. J. Staszewski and K. Worden, "The analysis of chaotic behaviour using fractal and wavelet theory", *Proc. Int. Conf. on Nonlinearity, Bifurcation and Chaos, Lodz, Poland*, 234 – 238 (1996).
13. W. J. Staszewski, "Identification of damping in MDOF systems using time-scale decomposition", *J. Sound Vibr.*, 203, 283 – 305 (1997).

14. W. J. Staszewski, "Wavelet based compression and feature selection for vibration analysis", *J. Sound Vib.*, 211, 735 – 760 (1998).
15. D. Coca and S. A. Billings, "Continuous-time system identification for linear and non-linear systems using wavelet decomposition", *Int. J. Bifur. Chaos*, 7, 87 – 96 (1997).
16. C.-H. Lamarque, S. Pernot, A. Cuer, "Damping identification in multi-degree-of-freedom systems via wavelet-logarithmic decrement-Part 1: theory", *J. Sound Vib.*, 235(3), 361 – 374 (2000).
17. R. Ghanem and F. Romeo, "A wavelet-based approach for model and parameter identification of non-linear systems", *Int. J. Nonl. Mech.*, 36(5), 835 – 859 (2001).
18. I. Antoniou, V. V. Ivanov, V. V. Ivanov, P. V. Zrelow, "On the log-normal distribution of network traffic", *Physica D*, 167(1-2), 72 – 85 (2002).
19. G. Y. Luo, D. Osypiw, M. Irl, "Vibration modelling with fast Gaussian wavelet algorithm", *Adv. Eng. Software*, 33(4), 191 – 197 (2002).
20. W. Glabisz, "Stability of one-degree-of-freedom system under velocity and acceleration dependent nonconservative forces", *Comp. & Structures*, 79(7), 757 – 768 (2001).
21. K. Hackl, "Wavelet based algorithms for elastoplastic shells", *Proc. of the 6th Conf. Shell Structures, Theory and Applications, Gdańsk, Jurata, Poland, October 12 – 14, 1998*, 137 – 138 (1998).
22. C.-H. Lamarque and J. M. Malasoma, "Analysis of nonlinear oscillations by wavelet transform: Lyapunov exponents", *Nonl. Dyn.*, 9, 333 – 347 (1996).
23. I. Daubechies, "Orthonormal bases of compactly supported wavelets", *Comm. Pure Appl. Math.*, 61, 909 – 996 (1988).
24. V. Perrier and C. Basdevant, "La décomposition en ondelettes périodiques, un outil pour l'analyse de champs inhomogènes: théorie et algorithmes", *La Recherche Aérospatiale*, 3, 53 – 67 (1989).
25. S. Pernot and C.-H. Lamarque, "A Wavelet-Galerkin procedure to study time-periodic systems: transient vibrations and stability analysis", *J. Sound Vib.*, (to appear).
26. S. Mallat, "A theory for multiresolution signal decomposition: the wavelet representation", *IEEE Trans. Patt. Anal. Math. Int.*, 11, 674 – 693 (1989).
27. S. Mallat, "Multiresolution approximations and wavelet orthonormal bases of  $L^2(\mathbb{R})$ ", *IEEE Trans. Patt. Anal. Math. Int.*, 315, 69 – 87 (1989).
28. Y. Meyer, *Ondelettes et opérateurs I: Ondelettes* (Actualités mathématiques, Hermann, Paris) (1990).
29. Wei-Zhang, L. Zhao, Y. Pei, "Global dynamics of a parametrically and externally excited thin plate", *Nonl. Dyn.*, 24, 245 – 268 (2001).
30. I. Lasiecka, "Finite dimensionality and compactness of attractors for von Kármán equations with nonlinear dissipation", *Nonl. Differ. Eq. Appl.*, 6, 437 – 472 (1999).
31. V. A. Krysko, J. Awrejcewicz, V. Bruk, "The existence and uniqueness of solution of one coupled thermo-mechanics problem", *J. Appl. Anal.*, 8(1), 129 – 139 (2002).
32. V. A. Krysko, J. Awrejcewicz, V. Bruk, "On the solution of a coupled thermo-mechanical problem for non-homogeneous Timoshenko-type shells", *J. Math. Anal. Appl.*, 273(2), 409 – 416 (2002).
33. J. Awrejcewicz, V. A. Krysko, A. V. Krysko, "Spatial temporal chaos and solitons exhibited by von Kármán model", *Int. J. Bifur. Chaos*, 12(7), 1465 – 1513 (2002).
34. J. Awrejcewicz and V. A. Krysko, *Nonclassical Thermoelastic Problems in Nonlinear Dynamics of Shells*, Springer-Verlag, Berlin (2003).
35. N. M. Afanas'eva, "Wavelet analysis: spectral analysis of local perturbations (theory and application)", *Izviestia VUZ, Nonl. Dyn.*, 2, 3-39 (1996) (in Russian).
36. C. Chui, "Wavelet analysis and its applications, Vol. 1. An introduction to wavelets., Vol.2. Wavelets: A tutorial in theory and applications.", Academic Press, San Diego (1992).
37. J. M. Combes, A. Grossmann, P. Tchamitchian, "Wavelets: time-frequency methods and phase space" Proceedings of the International Conference, December 1987: Marseille, France, Springer-Verlag, Berlin, New York (1990).
38. R. Coifman, Y. Meyer, S. Quake, M. Wickerhauser, "Signal processing and compression with wavelet packets", *Progress in wavelet analysis and applications* (Editions Frontières, Paris) 77 – 93 (1993).
39. M. Holschneider, *Wavelets: an analytical tool*, Clarendon Press, Oxford, New York (1995).
40. P. Lemarié, *Ondelettes et opérateurs I: Ondelettes*, Actualités mathématiques, Hermann, Paris (1990).
41. P. Lemarié, *Ondelettes et opérateurs II: Opérateurs de Calderón-Zygmund*, Actualités mathématiques, Hermann, Paris (1990).
42. P. Lemarié, *Ondelettes et algorithmes concurrents*, Actualités scientifiques et industrielles, Hermann, Paris (1992).
43. Y. Meyer and R. Coifman, *Ondelettes et opérateurs III: Opérateurs multilinéaires*, Actualités mathématiques, Hermann, Paris (1991).
44. Y. Meyer and R. Ryan, *Wavelets: Algorithms and applications*, SIAM, Philadelphia (1993).
45. A. Arneodo, G. Grasseau, M. Holschneider, "Wavelet transform of multifractals", *Phys. Rev. Lett.*, 61(20), 2281 – 2284 (1988).
46. G. Battle, "A block spin construction of ondelettes. Part 1. Lemarié functions", *Commun. Math. Phys.*, 110, 607 – 615 (1987).



47. G. Beylkin, R. Coifman, V. Rokhlin, "Fast wavelet transforms and numerical algorithms", *Comm. Pure Appl. Math.*, 44, 141 – 183 (1991).
48. S. Collineau and Y. Brunet, "Detection on turbulent coherent motions in a forest canopy. Part I. Wavelet analysis", *Boundary-Layer Meteorology*, 64(4), 357 – 379 (1993).
49. M. Farge, "Wavelet transforms and their applications to turbulence", *Annu. Rev. Fluid Mech.*, 24, 395 – 457 (1992).
50. C. Grebogi and J. A. Yorke, "Crises, sudden changes in chaotic attractor and transient chaos", *Physica D*, 181 – 200 (1983).
51. T. von Kármán, "Encyklopedie Der Math. Wiss." IV(4), Teubner, Leipzig, 311 – 385 (1908).
52. P. Lemarié, "Ondelettes à localisation exponentielle", *J. de Math. Pures Appl.*, 67, 227 – 236 (1988).
53. C. Maneveau, "Analysis of turbulence in the orthonormal wavelet representation", *J. Fluid Mech.*, 232, 469 – 520 (1991).



## JAN AWREJCIEWICZ

Jan Awrejcewicz received the M.Sc. and Ph.D. degrees in a field of Mechanics from the Łódź Technical University in 1977 and 1981, respectively. He earned also his bachelor's degree in Philosophy in 1978 from the Łódź University, and Doctor of Science degree in Mechanics from the Technical University of Łódź in 1990. He is author or co-author of 300 publications in scientific journals and conference proceedings, monographs (25), text books (2), edited volumes (2), conference proceedings (9), journal special issues (3), and other books (5) and other short communications and unpublished reports (130). He is now the Head of Department of Automatics and Biomechanics, and the Head of Ph.D. School on 'Mechanics'

associated with the Faculty of Mechanical Engineering of the Technical University of Łódź. In 1994 he earned the title of Professor from the President of Poland, Lech Wałęsa, and in 1996 he obtained the golden cross of merit from the next President of Poland, Aleksander Kwaśniewski. He is a contributor to 45 different research journals and to 100 conferences. During his scientific travel he visited 40 different countries. His papers and research covers various disciplines of mathematics, mechanics, biomechanics, automatics, physics and computer oriented sciences.

Technical University of Lodz (Poland)

Saratov State University, Saratov ( Russia)

Поступила 12. 05. 2003

---

From the Editorial Board: The article corresponds completely to submitted manuscript.